Tampere University

Aleksi Saarilahti

CALIBRATION OF PRICING MODELS TO BITCOIN OPTIONS

Master of Science Thesis
Faculty of Management and Business
Examiners: Professor Juho Kanniainen
Postdoctoral Researcher Anubha Goel
May 2023

ABSTRACT

Aleksi Saarilahti: Calibration of pricing models to bitcoin options
Master of Science Thesis
Tampere University
Master's Degree Programme in Industrial Engineering and Management
May 2023

A type of derivatives, which use crpytocurrency as an underlying asset has become more popular during the past years as they offer alternative solutions to traditional financial instruments. Even though the dynamics and pricing principles of different financial derivatives have been rather popular subjects in quantitative finance, the literature on crypto derivatives has been rather scarce. The calibration of the pricing model is often considered an essential part of the derivative pricing, aiming to find the optimal parameters of a certain model through the pricing data available. This is typically done by using the quoted market prices or quoted implied volatilities. Even though the obtained parameters are primarily for pricing purposes, they also give valuable information about the characteristics of the underlying asset.

The purpose of this thesis is to conduct a calibration of asset pricing models to the European-style call options, which use the bitcoin as an underlying asset. The option data involved was acquired from the Deribit cryptocurrency exchange from the review period of September 30th 2021 to October 31st 2021. With respect to the model calibrations, the stochastic volatility models of Heston and Bates are applied here. The calibrations of both models are carried out once per day across the review period by applying implied volatilities. With each calibration, a quoted implied volatility surface is established to which the model is calibrated. The study aims primarily at analysing the calibrated parameters and their development throughout the review period. On top of that, this study aims at answering what kind of implied volatility surfaces European-style bitcoin call options develop, and how these change across the review period.

Based on the calibration results both models produce relatively good implied volatility surface fits, especially for short maturities. The obtained parameters support the volatile behaviour of bitcoin and the positive correlation between returns and volatility, which is not uncommon in the crypto markets. The results also show that certain parameters have a more significant impact on the final outcome. Despite a few exceptions, the parameters remain rather stable across the review period. Based on the established implied volatility surfaces, the variation throughout the review period is relatively large. However, when comparing the formed implied volatility surfaces to the ones found in previous studies and literature, many similarities can be found. During the review period, each IV surface provides a rather clear smile effect at short time to maturities, but there is a tendency of a forward skewed shape when maturities increase. This also highlights the growing demand of OTM- options in order to better hedge the price risk of bitcoin.

Keywords: model calibration, bitcoin, implied volatility surface, option pricing, stochastic volatility models

TIIVISTELMÄ

Aleksi Saarilahti: Hinnoittelumallien kalibraatio bitcoin-optioille
Diplomityö
Tampereen yliopisto
Tuotantotalouden diplomi-insinöörin tutkinto-ohjelma
Toukokuu 2023

Kryptovaluuttoja kohde-etuutena käyttävät johdannaiset ovat yleistyneet viime vuosina merkittävästi tarjoten vaihtoehtoisia ratkaisuja tyypillisten rahoitusinstrumenttien rinnalle. Vaikka erilaisten johdannaisten dynamiikka sekä hinnoittelu ovat olleet erityisen suosittuja aiheita kvantitatiivisessa rahoituksessa, kryptojohdannaisia on kuitenkin tutkittu vielä suhteellisen vähän. Keskeistä johdannaisten hinnoittelussa on hinnoittelumallin kalibrointi, jossa kyseisen mallin optimaalisia parametreja pyritään selvittämään markkinoilta saatavan hinnoitteludatan avulla. Tyypillisesti kalibrointi suoritetaan käyttäen joko johdannaisten rahamääräisiä hintoja tai vaihtoehtoisesti niiden implisiittisen volatiliteetin arvoja. Vaikka kalibroidut parametrit ensisijaisesti helpottavat hinnoittelumallien käyttöä, ne antavat myös arvokasta tietoa kohde-etuuden käyttäytymisestä.

Tämän tutkimuksen tavoitteena on toteuttaa hinnoittelumallien kalibrointi eurooppalaisille optioille, joiden kohde-etuutena on bitcoin. Kyseinen optiodata ladattiin Deribit-kryptovaluuttapörssistä ja se sijoittui tarkasteluvälille 30.9. - 31.10.2021. Kalibroitaviksi malleiksi valikoituvat stokastisen volatiliteetin mallit Heston ja Bates. Molemmat mallit kalibroidaan jokaisena tarkasteluperiodin päivänä. Jokaisen päivän osalta bitcoin-optioille muodostetaan myös implisiittiset volatiliteettipinnat, joita vasten hinnoittelumallien kalibraatiot toteutetaan. Tutkimuksessa pyritään ensisijaisesti analysoimaan kalibroituja parametreja sekä niiden kehittymistä tarkasteluperiodin aikana. Toissijaisesti työ pyrkii vastaamaan, minkälaisia implisiittisiä volatiliteettipintoja eurooppalaiset bitcoin-optiot muodostavat ja kuinka ne kehittyvät tarkasteluperiodin aikana.

Saatujen tulosten perusteella molemmat hinnoittelumallit tuottavat kohtalaisen hyvän sovitteen markkinoilta havaitun implisiittisen volatiliteettipinnan kanssa, erityisesti kun maturiteetit ovat lyhyitä. Saadut parametrit tukevat bitcoinin volatiilia käytöstä sekä positiivista korrelaatiota tuottojen ja volatiliteetin välillä, joka on tyypillistä kryptomarkkinoilla. Tuloksista havaitaan myös, että tietyillä parametreilla on selvästi suurempi vaikutus lopputuloksen kannalta. Pääosin parametrit pysyvät tasaisina läpi tarkasteluperiodin muutamaa poikkeusta lukuun ottamatta. Muodostettujen implisiittisten volatiliteettipintojen osalta pinnat kokevat kohtalaisen paljon vaihtelua läpi tarkasteluperiodin. Tästä huolimatta pinnat kuitenkin tarjoavat monia yhtäläisyyksiä kirjallisuuden löydösten kanssa. Tarkasteluperiodin aikana implisiittiset volatiliteettipinnat muodostavat selvästi havaittavan hymy-efektin lyhyiden maturiteettien osalta, mutta pinnat tyypillisesti vinoutuvat eteenpäin maturiteetin kasvaessa korostaen miinusoptioiden voimistunutta kysyntää bitcoinin hintariskin hallitsemiseksi.

Avainsanat: mallien kalibrointi, bitcoin, implisiittinen volatiliteettipinta, optioiden hinnoittelu, stokastiset volatilitettimallit

PREFACE

Preparing this thesis has been my final battle for a long time and I am extremely happy to finally bring this battle to the end. I would like to express my honest gratitude to my supervisor Juho Kanniainen for the professional guidance during the whole process. This thesis has been easily the most demanding part of my studies, but also one of the most rewarding parts of it. I would like to thank Maria Saraketo, who has been my biggest supporter bringing a lot of hope and happiness to my days. Special thanks also to Kim Studenski and Hanna Saraketo for giving valuable comments and insights to my thesis.

In the beginning of my studies I couldn't even imagine where the next years would take me. Thanks to all my friends for the many unforgettable moments we had during these past years. Finally, I am grateful for my family for always believing in me and supporting my goals.

All in all, many new experiences, friends and challenges later it is time to turn a new chapter in life and focus on the upcoming golf season.

Helsinki, 18th May 2023

Aleksi Saarilahti

CONTENTS

LIST OF SYMBOLS AND ABBREVIATIONS

BS	Black-Scholes
BTC	bitcoin
C_t	price of the European-style call option
$IV - MSE$	implied volatility mean squared error
IVS	implied volatility surface
K	strike price
M	moneyness of $log\ S/K$ describing whether an option is either in the money, at the money or out of the money
P_t	price of the European-style put option
$S\&P\ 500$	Standard & Poor's 500 index including 500 of the biggest US companies
S_t	asset price
T	time to maturity
δ	standard deviation of the jump size
η	volatility of volatility
κ	mean reversion speed of variance
λ	jump intensity
μ	expected rate of return
$\overline{k}$	mean jump size
ρ	correlation between the Wiener processes of W_t^1 and W_t^2
σ	volatility
θ	long-term variance
$\widehat{\sigma}$	implied volatility
r	risk-free rate
v_0	initial variance
v_t	variance

1. INTRODUCTION

1.1 Background

Financial markets have been changing rapidly over the past decades. Innovative solutions and more complicated financial instruments have been issued into markets and new participants have become involved in the financial ecosystem. The change has been notably driven by the revolutionary development of technology allowing the transition towards the digital realm. One of the greatest innovations within the financial market has been cryptocurrencies operating through blockchain technology. Together, crypto assets and blockchain have created one of the fastest growing industries as summarized by Lipovyanov (2019, p. 5).

The first versions of digital currencies have appeared already in the 1980s (e.g. Chaum, 1983). However, those did not gain much ground since they were not able to solve a fundamental issue within a digital cash environment relating to double-spending. During the global financial crisis in 2008 the cryptocurrency environment changed for good, when Satoshi Nakamoto (2008) released a theoretical ideology about blockchain technology and its capabilities in decentralized networks, known as bitcoin. A year later, the actual bitcoin was released when Satoshi made the first transaction, which was added to the first block of the bitcoin blockchain.

Nowadays, with hundreds of forms of digital currencies in the financial market, bitcoin appears to be far more superior in terms of its applicability compared to other cryptocurrencies (Mir, 2020). Bitcoin's popularity is not alone attributable to an individual characteristic, but rather is the sum of several factors. To mention a few of these, the bitcoin environment operates without a central authority, making it completely independent (Lipovyanov, 2019, p. 28). Even though anyone can get involved in the bitcoin blockchain, it still allows a safe place for funds without revealing the identity of the participant. Bitcoin has also gained ground within portfolio management since it has provided comparable results to those with gold (Härdle et al., 2020). Although Gkillas and Longin (2019) refer to bitcoin as "the new digital gold", bitcoin's price volatility has been shocking over the past few years compared to gold.

Since bitcoin prices have suffered from a relatively high volatility, it has increased the

need for hedging and managing the risk exposure of bitcoin (Borri, 2019) accelerating the demand of bitcoin derivatives (Zulfiqar and Gulzar, 2021). A noteworthy landmark in the development of cryptocurrency derivatives was related to the induction of bitcoin futures in 2017 (Jalan et al., 2021). A few years later, European-style bitcoin options were released making the hedging process even more flexible. However, the release of new derivatives gives a reason to challenge the traditional derivative pricing models and fundamentals which affect the pricing. Since a derivative pricing model should describe the price movements of an underlying asset, it becomes rather interesting to evaluate the valuation dynamics of derivatives that use the bitcoin as the underlying asset.

In the literature, a relatively lot of research has been published on the fundamentals of the bitcoin price. However, the literature on the valuation of bitcoin derivatives is still quite narrow. A few studies on the subject, such as Cao and Celik (2021) and Jalan et al. (2021), have highlighted that the valuation dynamics of bitcoin derivatives driven by the extreme volatile and uncertain behaviour are still rather unclear. In other words, there is not an accurate pricing model to establish the fair value of cryptocurrency derivatives in a consistent fashion.

The applicability of a certain pricing model can be evaluated through the model calibration. The model calibration refers to a process where the parameters of a pricing model are defined in a way that the model outputs replicate as closely as possible with the observable outputs from the market (Büchel et al., 2022). The obtained parameters are known as true parameters being used when the actual pricing will be done with the calibrated model. The more accurate the calibration results are, the more valid the predictability of a pricing model is. Even though the model calibration represents a high-value tool from a pricing perspective, it also provides essential information about the characteristics of the underlying asset.

A suitable model alone does not guarantee good calibration results. As highlighted by Escobar and Gschnaidtner (2016), the results are also affected by other calibration-related aspects, such as the applied optimization algorithm, loss function and initial parameters. Usually, the model calibration has been carried out through the quoted prices or implied volatilities. Especially with the latter one, the model calibration can be done against the quoted implied volatility surface, which makes it even easier to evaluate the characteristics of the underlying asset.

Despite the growing availability of bitcoin options, the literature on the implied volatility dynamics of bitcoin can be considered rather limited. In association with the topic in question, Hou et al. (2020) and Zulfiqar and Gulzar (2021) have evaluated the characteristics of bitcoin through the implied volatilities. They came across many similarities compared to the equity market and made interesting findings about the sentiments of the bitcoin traders.

1.2 Objective and structure of the study

The purpose of this thesis is to conduct a calibration of asset pricing models to the European-style call options, which use the bitcoin as an underlying asset. The option data is based on the Deribit cryptocurrency exchange from the review period of September 30th 2021 until October 31st 2021. With respect to the model calibrations, we apply two option pricing models introduced by Heston (1993) and Bates (1996). The Heston model can be considered a classic stochastic volatility model whereas the Bates model represents an extension of the Heston model with an additional jump diffusion part in the price process.

The calibrations of both models are carried out once per day across the review period by applying implied volatilities. With each calibration, a quoted implied volatility surface is formed to which the model is calibrated. This thesis aims to cover the following research questions keeping the main focus on the latter one:

1. What kind of implied volatility surfaces do European-style bitcoin call options develop, and how do those change across the review period?
2. What kind of parameters and mean squared errors are obtained when the Heston and Bates asset pricing models are calibrated against quoted implied volatility surfaces, and how do those parameters and mean squared errors develop throughout the review period?

This study is structured in the following manner. Chapter two briefly summarizes insights from the literature related to cryptocurrencies, keeping the main focus on bitcoin. This is followed by an insight into the pricing of European-style call options through the Heston and Bates models in chapter three. That same chapter includes a brief breakdown of option pricing through the fast Fourier transform and the basic concepts of implied volatility derivation. The chapter concludes with a discussion about the selection of the models.

Chapter four introduces the main features of a model calibration process, the Nelder-Mead algorithm as well as standard errors and stabilities of model parameters. Furthermore, the illustrative effects of changing parameters are explained. Chapter five gives a short introduction to the research process as well as data acquiring and processing. Also, that same chapter looks at the main assumptions related to the empirical part and includes the considerations about the reliability and validity of the results.

In chapter six, the empirical results about the calibrations and implied volatility surfaces are introduced and discussed. At the end of the thesis, the main findings based on the empirical results are summarized.

2. CRYPTOCURRENCY

This chapter briefly summarizes relevant insights from the literature related to cryptocurrencies. As the data applied in this thesis is based on bitcoin options, the chapter will give a more comprehensive overview over literature related to bitcoin. At the end of the chapter, the findings about the bitcoin price dynamics are introduced shortly.

It is important to note that the exact background of the technicalities of bitcoin are beyond the scope of this thesis. However, the topic in question is summarized shortly within this chapter to provide a necessary understanding for the subject and this thesis itself.

2.1 Establishment of cryptocurrencies

For a long time, fiat currencies have been at the heart of modern monetary policy. According to Dorn (2017, p. 1), a new era began in August 1971 when President Nixon enacted a plan that foreign central banks were not allowed to freely convert their dollars for gold at the official exchange rate. At about the same time numerous national central banks started to implement a more comprehensive monetary policy to control the money supply within their economies. A widely accepted theme of regulated monetary policies has been inflation targeting, which however, has had somewhat varying degrees of success over the years and across different countries. (Lipovyanov, 2019, p. 23).

Fiat money represents a type of currency that is issued by a government without having intrinsic value since it is not backed by anything (Mir, 2020). In the fiat environment, as explained by Franco (2014, p. 5), there is a government decree declaring the currency to be a legal tender. In other words, a government concludes whether some payment will be recognized as a trade settlement in a country. The Euro and the US dollar are good examples of fiat currencies being usually applied in global trade, as both of these currencies represent large and very credible economies in the world.

Regardless of the popularity of the fiat system, there are some contradictory issues within the fiat-based environment. Based on Mir's (2020) study, the fiat system suffers from a lack of privacy as intermediaries, such as commercial banks, have to maintain a lot of personal information about their customers. Furthermore, that information is usually shared with other authorities. The author also emphasizes the vulnerability to economic

and political situations since global crises between big economies are reflected in the value of the fiat currency (Mir, 2020). Lipovyanov (2019, p. 17) highlight similar issues about the weak fiat systems being exposed to economic uncertainty. They further note that these kind of difficulties may at worst lead to hyperinflation where the value of a certain currency falls enormously, as happened in Zimbabwe in 2007 (Lipovyanov, 2019, p. 17).

Several factors, such as a need to deal with the uncertainty in the existing economy (Raj, 2019, p. 12), have accelerated the evolutionary steps towards digital cryptocurrencies driven by blockchain technology. A digital currency itself was not so much a new concept, but the concept of an open-source currency without the need for a central authority was revolutionary, as noted by Härdle et al. (2020).

According to Härdle et al. (2020), a cryptocurrency represents a digital asset that uses blockchain technology to control, secure and verify its transactions. The blockchain technology is based on a distributed network and hence it is usually referred to as distributed ledger technology (more details will be presented in Section 2.2). While the fiat currencies are regulated and controlled by the irrational governments and central banks, cryptocurrencies are based on purely science, programming and mathematics, as highlighted by Lipovyanov (2019, p. 20).

It should be noted that nowadays there exists a large number of different cryptocurrencies, each with their specific set of principles and rules. As Mir (2020) debates, this is partly attributable to the fact that people are becoming more and more familiar with the new digital form of money and starting to move their interests towards cryptocurrencies. They noted that people are especially attracted by the high security of cryptocurrencies and their capabilities to execute relatively fast online transactions. Even though the past few years have revealed a lot of curiosity about cryptocurrenices, the transactions are still mostly executed by denominating them at first in the fiat currency as concluded by Lipovyanov (2019, p. 20).

In the beginning, digital payment methods and currencies required a trusted third-party intermediary, for example MasterCard, to execute the transaction. In order to operate without third parties, an uncomplicated way to create digital value is to issue value to a certain data pattern, such as a string form of binary numbers. However, this approach includes a problem called double-spending. The double-spending problem relates to information of currencies that can be replicated very easily at barely any cost, which predisposes cryptocurrencies to scams and criminal activities. Until the release of bitcoin, the double-spending problem was present and digital payment methods and currencies were mostly handled through third party intermediaries. (Franco, 2014, p. 11-13)

2.2 Bitcoin and blockchain

The idea of bitcoin was invented in 2008 based on Satoshi Nakamoto's (2008) theoretical ideology about blockchain technology and its capabilities in decentralized networks. A year later, the actual bitcoin was released when Satoshi made the first transaction, which was added to the first block of the bitcoin blockchain. The first block is more familiarly referred to as the genesis block and later it has become the proof of blockchain's legitimacy. (Raj, 2019, p. 10)

Bitcoin was the first cryptocurrency solving the problem of double-spending in a decentralized way (Raj, 2019, p. 10). The establishment of the bitcoin could not have come at a better time since bitcoin's launch during the global economic and financial crisis in 2008 and 2009 was one of the most meaningful things to ever happen in the modern monetary history, as argued by Lipovyanov (2019, p. 22).

Bitcoin revolutionized the era of digital currencies as it was the first cryptocurrency which was not controlled or packed by any individual entity or country (S. Zhang et al., 2019). That means bitcoin is purely decentralized and there is no institution, person or central server behind it (Franco, 2014, p. 3-4). Ever since bitcoin was released, it has attracted a lot of interest among people. As noted by Franco (2014, p. 6-8), this is partly driven by the fact that bitcoin is an open-source software. The open-source software makes the established source code accessible for anyone to modify, use or develop it for free. This has given rise to many alternative cryptocurrencies as well.

Bitcoin itself is a rather complex entity and describing all its features would fall out of the scope of this thesis. However, the topic in question is summarized shortly below to provide the necessary understanding for the subject and this thesis itself. As supported by Lipovyanov (2019, p. 37), in the big picture bitcoin's main fundamentals can be divided into four different topic areas: (i) blockchain or distributed ledger technology (DLT), (ii) peer-to-peer network, (iii) cryptography and (iv) proof-of-work consensus algorithm.

The foundation of the entire bitcoin decentralized system is the blockchain technology. As stated by Franco (2014, p. 95), in essence blockchain refers to a distributed database holding all the bitcoin transactions since the beginning. The author also stated that blockchain represents a method to secure this database (Franco, 2014, p. 95). According to Lipovyanov (2019, p. 38), blockchain consists of blocks and each block represents a type of data structure including transaction records and a link between the blocks (hash). Note that old transactions (blocks) are never removed from the chain and hence a blockchain can only increase in length as noted by Franco (2014, p. 105).

A blockchain is distributed across a wide computer network and therefore it is also called a distributed ledger. Each computer in the network holds the same information related to a series of transactions. (Lipovyanov, 2019, p. 38) This network is more familiarly known

as a peer-to-peer network (P2P), which removes extra intermediaries and establishes trust between unknown parties. Based on Raj (2019, p. 80-81), a P2P network means a network where groups of autonomous computers (nodes) are connected and equally privileged, being open to everyone. The P2P network shares information without any centralized servers.

When considering the concept about a network available to everyone, it also exposes the system to greater risks. This brings up the next key element in bitcoin design called cryptography. Cryptography can be considered a somewhat extensive topic but according to Lipovyanov (2019, p. 44), cryptography represents the science of secure communication that is used to protect all kinds of private information from falling into the wrong hands. Based on Raj (2019, p. 23) the fundamental objective of cryptography is to allow two participants to communicate over an unsecure environment by encrypting the information from the sender to a form that can only be decrypted by the receiver.

There are several cryptography approaches in the bitcoin environment but a few of them rise above the rest. As one example Lipovyanov (2019, p. 44) highlights the meaning of private and public keys. As defined by Franco (2014, p. 53), the public key is applied by the sender to protect and encrypt data relating to the transaction. The receiver can then decrypt the transaction data by using the personal private key generated by a user's bitcoin wallet software. Note that the private key must not be given to others since it provides access to the user's bitcoins on the blockchain. Regardless of the several cryptography methods, the most important approach in the bitcoin system is known as hashing, which is considered one of the most commonly applied primitives of cryptography as argued by Raj (2019, p. 26).

A hash function is an algorithm that applies information of arbitrary length as an input resulting in a string as an output, called the hash value (Franco, 2014, p. 95). Within the bitcoin environment, hashing is used in the blockchain to establish an identity string for each of the blocks by computing their hash values. Each block consists of the hash value of the previous block and hence they form a chain of blocks. (Raj, 2019, p. 48) Furthermore, hashing and hash functions represent very essential parts of the bitcoin system since they create the basis of the bitcoin's proof-of-work consensus as emphasised by Lipovyanov (2019, p. 50).

Proof-of-work (PoW) can be considered as a consensus algorithm to prove that a single node has actually done some work to establish a new block of the blockchain (Raj, 2019, p. 10). The proof-of-work consensus plays an essential part in the bitcoin ecosystem since each transaction is validated through the proof-of-work by solving the cryptographic hash puzzles. In other words, bitcoin applies cryptographic hash functions introduced previously to carry out the proof-of-work mechanism as noted by Franco (2014, p. 96).

These elements alone do not make bitcoin exceptional, but together they allow the pro-

cess of updating and maintaining the transactions of the blockchain known as mining. Conclusively, mining refers to the process where each transaction is verified and added to the blockchain. The participants involved in this process are called miners (Küfeoğlu and Özkuran, 2019).

According to Lipovyanov (2019, p. 55-60), the mining process starts when the miners gather new transaction data. After receiving such data, each miner verifies every transaction against a long list of criteria. After these verified transactions are gathered to the memory pool, a space for valid but still unconfirmed transactions. Next, miners aggregate the transactions in a candidate block with certain information, such as a creation timestamp, derived through hash functions resulting in a unique digital fingerprint. However, all the necessary information is not known and thus peers of the bitcoin network need to compete against each other through the proof-of-work by solving the cryptographic hash puzzles. The first miner who manages to compute a hash for the new block, i.e. finds a solution to the proof-of-work puzzle, gets the right to add a new block and update the ledger of pending transactions. The new block is shared to everyone on the network and each node needs to verify the block to make sure there is nothing wrong with it. Finally, each node updates the copy of the new block in their own blockchain.

Moreover, the miner who successfully managed to solve the puzzle receives a reward of a fixed amount of bitcoins and all transaction fees attached to the transaction as a compensation for the consumed time (Härdle et al., 2020). Actually, these gained rewards are the only way to release new bitcoins into circulation. Therefore, mining is also referred to as a process of making new bitcoins as stated by Küfeoğlu and Özkuran (2019).

According to Franco (2014, p. 107-108), the mining process for one block takes around 10 minutes on average. The author also noted that the reward gained from the verification task will be halved every 210 000 blocks taking roughly 4 years. Since the reward is exponentially decreasing, the total number of bitcoins will settle to 21 million coins. However, this is estimated to happen in 2140 at the earliest writes Raj (2019, p. 260). When the total number of bitcoins is reached, the reward for the miners includes only the transaction fees of bitcoins.

2.3 Dynamics of bitcoin price

Bitcoin's price development has been explosive during the past years (Figure 2.1). Between the years 2015 and 2017, the evolution of bitcoin's price was rather stable and the price was varying mostly between USD 200 and USD 1 000. However, in the beginning of 2017, the popularity of cryptocurrencies increased rapidly and the price almost reached the level of USD 20 000 at the end of 2017. This had implications for the entire bitcoin environment and for example accelerated the evolution of the bitcoin mining industry according to De Vries (2020). Since 2017, the price of bitcoin has been varying a lot, the

highest peak so far was seen in November 2021 when the price exceeded the level of USD 65 000. At the time of writing this thesis in March 2023, the price has been around USD 24 000 with a market capitalization of over USD 500 billion based on the CoinDesk's BTC price index (CoinDesk, n.d).

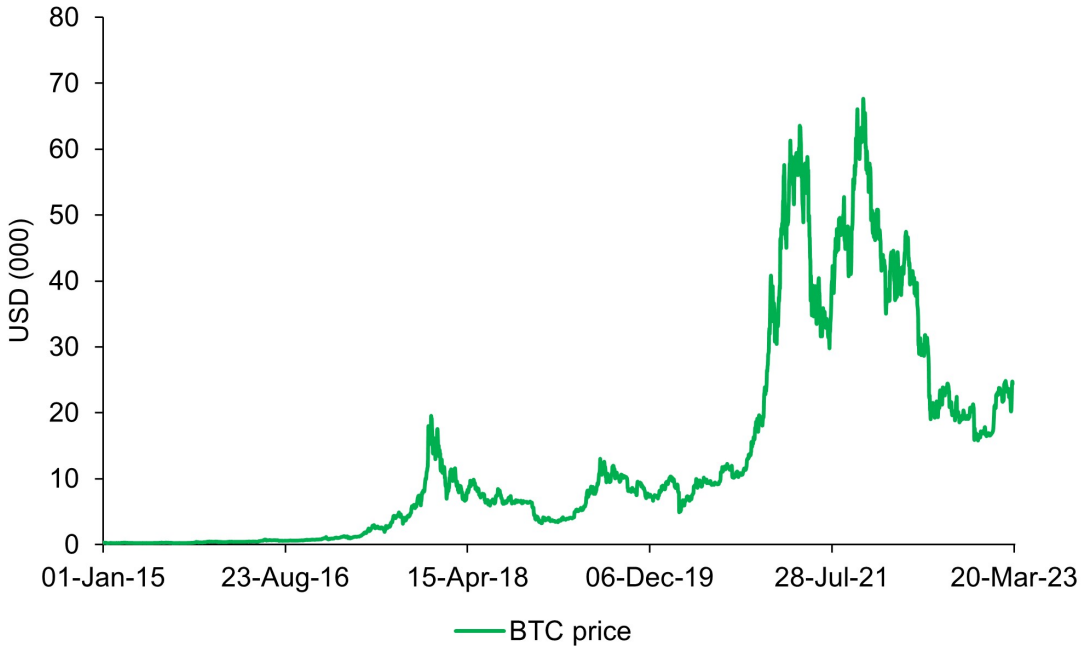

Figure 2.1. *BTC price development from the 1st of January 2015 to the 20th of March 2023 (CoinMarketCap, n.d).*

Ever since the first bitcoin transaction was recorded in 2009, the drivers explaining bitcoin's price have become a somewhat trending topic among practitioners. To mention a few of them, for example, Hayes (2017) and Bhambhwani et al. (2019) have examined on how certain drivers such as the rate of unit production, computing power and network size impact on bitcoin's price. Furthermore, while Athey et al. (2016) tried to develop a framework for pricing bitcoin, Aste (2019) investigated the connection between the bitcoin price and investor sentiments.

However, even though there exists a lot of research on the subject, the fundamental value of bitcoin and the factors driving its price are still rather unclear and not widely acknowledged as noted by various scholars (W. Zhang et al., 2021; Alexander, Deng, et al., 2022). In comparison with more traditional equity assets, bitcoin does not have similar price fundamentals, such as simple cash flows or dividends, which could be applied in determining the fair market price. Instead, bitcoin reminds more of a physical commodity, such as gold, whose price is driven by supply and demand as well as the ability to maintain its value over time. (Santos-Alborna, 2021, p. 41)

When looking at Figure 2.1, it's rather easy to conclude how volatile bitcoin really is. This is supported by several studies in the literature, one of which is Hou et al. (2020) arguing

that the bitcoin's price behaviour is clearly more volatile in comparison to stocks. Hou et al. (2020) also highlight that both the bitcoin prices and returns are very sensitive to big news and events in the market. Note that there is not one individual factor alone making bitcoin incredibly volatile, but it is rather related to many separate factors such as its unregulated microstructure that allows everyone to take part (Lipovyanov, 2019, p. 6) and its rather complex mining dynamic (Santos-Alborna, 2021, p. 48).

Since bitcoin has suffered from a relatively high volatility, it has increased the need for hedging and managing the risk exposure as noted by Borri (2019). Hence, this has accelerated the emergence of bitcoin derivatives. According to Jalan et al. (2021), a remarkable landmark in the development of cryptocurrency derivatives was related to the induction of bitcoin futures in 2017. Through the bitcoin futures, traders and institutional investors were able to hedge their positions for the first time against bitcoin's relatively high price risk.

The release of bitcoin derivatives offered a convenient way of short selling, and thus they accelerated the integration of bitcoin and traditional institutional investors by providing an efficient framework for trading purposes (Köchling et al., 2019). Later on, the hedging of cryptocurrency positions became more flexible with the release of options in bitcoin and ethereum. As highlighted by Hoang and Baur (2020) options have some advantages over futures as they tend to offer more maturity-strike combinations for hedging purposes.

Usually, bitcoin options have been considered as so-called inverse products since the possible payoff has been often denominated in bitcoins instead of some fiat currency. For instance, these types of inverse BTC options are provided by Deribit, which is considered one of the largest exchanges for crypto options. The characteristic of inverse bitcoin options has been explored more comprehensively by Alexander et al. (2021) and Teng and Härdle (2022). The authors conclude that BTC inverse options comply with slightly different pricing and hedging principles compared to standard options (Alexander et al., 2021; Teng and Härdle, 2022).

Bitcoin has also provided new diversification opportunities for portfolio management. As highlighted by Härdle et al. (2020) bitcoin has the prerequisites to replace gold in some situations since they have many similarities as both are dependent on mining and both have a finite supply. This is also supported by Gkillas and Longin (2019) who referred to bitcoin as "the new digital gold" which can represent an important role in asset management and provide comparable results as those with gold. Moreover, Y. Liu et al. (2022) reviewed several price and market drivers in the stock market and their counterparts within the cryptocurrency context. As a result, they identified some achievable and successful long-short strategies by applying cryptocurrencies.

Bitcoin and other cryptocurrencies have often been associated with arbitrage opportunities amongst scholars. As proposed by Makarov and Schoar (2020) and Krückeberg and

Scholz (2020), crypto traders are able to find considerable arbitrage possibilities within the bitcoin market. Based on Härdle et al. (2020), this is partly attributable to numerous cryptoexchanges with even more cryptocurrencies. Therefore, price deviations driven by market inefficiencies inherently exist. For example, bitcoin is one of the most liquid cryptocurrencies without having an agreement on the “spot” price. These observations are also supported by Bistarelli et al. (2019) who emphasized different cryptocurrency arbitrage strategies driven by the cryptoexchanges representing different prices.

3. OPTION PRICING

This chapter focuses on option pricing from a European call option perspective since the model calibrations within this thesis have been carried out to the European-style BTC call options. In general, options refer to a type of financial derivative allowing their owner the right, but not the obligation, to buy or sell the underlying asset at a given price by a certain date. When it comes to European-style options, those can be exercised only on their maturity date.

As highlighted in Section 2.3 bitcoin options have been usually considered as inverse products, since the possible payoff has been usually denominated in bitcoins instead of some fiat currency. However, in this thesis it is assumed that the option holder can convert the possible BTC option payoff immediately into the domestic currency. Therefore, the applied BTC options have been considered more like standard European-style options than inverse options.

In this study, the Heston and Bates asset pricing models have been applied. To give a comprehensive overview of these those models, the basic concepts of diffusion models and jump diffusion models will be introduced in this chapter. Furthermore, a brief breakdown of option pricing through the fast Fourier transform and the basic concepts of implied volatility will be provided below. Finally, the selection of the models is discussed.

3.1 Diffusion models

This section briefly illustrates the basic concepts of pricing models based on diffusion processes. As defined by Ratcliff and Tuerlinckx (2002), the diffusion process refers to a continuous variation of the discrete random walk process. The diffusion process is usually suitable with a certain situation where a given variable makes two-choice decisions. According to Kienitz and Wetterau (2013, p. 35), several well-known asset pricing models are based on the diffusion process. Those models are usually described through a stochastic differential equation which is satisfied by a Brownian motion (known as a Wiener process) representing a continuous stochastic process.

Based on Hull (2012, p. 280), stock prices are often assumed to comply with the Markov process. As defined by Ibe (2013, p. 49-52), the Markov Process can be considered a

certain type of stochastic process where the probability of each event is determined by the previous event. Hence, with respect to stock prices, the historical price development is impractical and irrelevant for estimating future prices since only the current stock price is meaningful for the future development. Furthermore, when a unit of time is close to zero and stock prices are assumed to comply with the Markov process, the stochastic process for the time unit resembles the Wiener process.

Below is a simple derivation of the Wiener process by following Hull (2012, p. 282-287). The variable z complies with the Wiener process if the following assumptions are satisfied:

1. The change of the variable z within a small period of time Δt can be described as:

$$\Delta z_t = \epsilon_t \sqrt{\Delta t}, \tag{3.1}$$

   where ϵ_t follows a standardized normal distribution with a mean of zero and a variance rate of 1. This means that Δz_t is a normally distributed random variable with mean of zero and standard deviation of $\sqrt{\Delta t}$.

2. The variable Δz_t complies with the Markov process introduced above. In other words, the values of Δz_t within short time intervals are independent.

In a stochastic process, a drift rate and variance rate refer to the mean change and variance per unit time. The basic Wiener process of Δz_t defined above has a drift rate of 0 and a variance rate of 1. Since the drift rate is zero, the future value of z at a given time t is equal to its current value. When the drift rate and the variance rate represent some other values, the Wiener process is called a Generalized Wiener process which can be described in terms of Δz_t for a certain variable x as follows:

$$dx_t = adt + bdz_t, \tag{3.2}$$

where a and b represent constant variables. Moreover, dz_t models a Wiener process of Δz_t when $t \to 0$. The term of adt represents the drift rate of a per unit of time for variable x. In a similar fashion, the term of bdz_t illustrates the variance rate which can be considered as an increased variability to the path movement followed by the variable x.

The generalized Wiener process assumes that the expected drift rate and variance rate are constant. Obviously, the constant drift rate is not appropriate since the expected rate of return is not independent of the asset's price. Hence the assumption about the constant drift rate is substituted by an assumption where the expected drift rate is divided by an asset price. If there is not any uncertainty that the variable of dz_t = 0, the equation for the asset price can be written in the following manner:

$$\Delta S_t = \mu S_t \Delta t, \tag{3.3}$$

where the S_t represents the asset price at a certain time t and μ means the asset's expected rate of return. Therefore, the μS_t implies the expected drift rate in the asset price of S_t. Within a short time period of Δt, the expected growth in the asset price of S_t can be represented as $\mu S_t \Delta t$. When Δt decreases towards zero, the previous equation can be described as follows:

$$dS_t = \mu S_t dt. \tag{3.4}$$

The equation can be presented alternatively as:

$$\frac{dS_t}{S_t} = \mu dt. \tag{3.5}$$

Undoubtedly, the development of an asset price includes some uncertainty making the variable $dz_t \neq 0$ which means that an investor is unaware of the expected rate of return regardless of whether the asset price is high or low. Now, when also taking the Wiener process of dz_t into account, it leads to the following equation:

$$dS_t = \mu S_t dt + \sigma S_t dz_t \tag{3.6}$$

or alternatively:

$$\frac{dS_t}{S_t} = \mu dt + \sigma dz_t, \tag{3.7}$$

where the variable σ represents the standard deviation of the asset price, referred to as volatility and σ^2 refers to the variance of the asset price. The equation defined above is one of the most applied dynamics for modelling the asset price behaviour. Note that equations of (3.6) and (3.7) assume a real world environment while the risk neutral environment is usually applied in asset pricing. Therefore, the expected rate of return μ is often modelled through a risk-free rate of r.

3.1.1 Black-Scholes model

The pricing process for European-style options changed for good in 1973 when Fisher Black and Myron Scholes introduced a new option pricing model called the Black-Scholes model (BS model) (Black and Scholes, 1973). The key suggestion behind the model was to eliminate the risk by applying a hedge strategy of buying and selling the underlying asset at the right time as highlighted by the scholars (Black and Scholes, 1973). It should be noted that the BS model has been considered one of the most remarkable models in the late history of modern finance. The basic concepts of the BS model will be briefly

introduced in this section as they provide the basis for the development of the Heston and Bates models.

The functionality of the BS model depends on several assumptions related to the pricing environment. Those are summarized clearly by Boyle and McDougall (2019, p. 86) in the following manner:

1. Asset prices are continuous and lognormally distributed. Moreover, the prices follow a geometric Brownian motion (i.e. Wiener process) with a constant expected return of μ and volatility of σ.
2. Assets can be sold short.
3. Assets are completely divisible without any taxes or trading costs.
4. Dividends do not exist on the underlying asset over the maturity of the option.
5. Markets are efficient and thus there are no arbitrage opportunities available.
6. The risk-free rate r is constant and equal for borrowing and lending actions.

The common solutions for the Black-Scholes differential equation (3.13) have been briefly illustrated here by following Hull (2012, p. 299-314). As mentioned before, the asset price process of the BS model follows the geometric Brownian motion, and thus it is consistent with the equation (3.6). Henceforth, let us denote the Wiener process as dW_t instead of dz_t. Driven by this, the diffusion equation (3.6) for the underlying price of S at time t can be given as follows:

$$dS_t = \mu S_t dt + \sigma S_t dW_t, \tag{3.8}$$

where μ is the expected rate of return (drift) and σ represents the volatility. It should be noted that the price process above is priced under a physical probability measure reflecting the situation, where investors would require more profit for higher risk. Therefore, the expected return should be adjusted with a certain appropriate risk premium when calculating the fair price of a derivative. Unfortunately, some of the derivatives are riskier than others leading to different risk premiums and providing undesirable arbitrage opportunities. Since the risk is somewhat difficult to quantify, the assets can be also priced under a risk-free probability measure instead of trying to separate the risk premiums for each investor. By applying the risk-free probability measure, it is assumed that financial markets are efficient and free from arbitrage opportunities. Furthermore, the price process (3.8) under the risk-free probability can be defined as follows:

$$dS_t = r S_t dt + \sigma S_t dW_t^*, \tag{3.9}$$

where variable r and dW_t^* refer to a risk-free rate and the Wiener process modified by

a risk-free probability measure. Overall, equations (3.8) and (3.9) are identical when the returns are discounted through the risk-free discount rate of r.

The defined price process (3.8) as such does not represent a very practical or applicable form to be used in option pricing. A well-known process for differential calculus is called Itô's lemma. Itô's lemma is based on Itô's (1951) study and it basically refers to an approach of modelling a stochastic process where both the function of some variable and the variable itself follow the stochastic process. By applying Itô's lemma, the price process (3.8) can now be presented in a way that f refers to the price of the derivative whereas S and t imply the asset price and time. When supposing that f is some function of variables S and t, the price process can be defined in the following manner:

$$df = \left(\frac{\partial f}{\partial S}\mu S + \frac{\partial f}{\partial t} + \frac{1}{2}\frac{\partial^2 f}{\partial S^2}\sigma^2 S^2\right)dt + \frac{\partial f}{\partial S}\sigma S dW_t. \tag{3.10}$$

The above equation can be also presented as a discrete version:

$$\Delta f = \left(\frac{\partial f}{\partial S}\mu S + \frac{\partial f}{\partial t} + \frac{1}{2}\frac{\partial^2 f}{\partial S^2}\sigma^2 S^2\right)\Delta t + \frac{\partial f}{\partial S}\sigma S \Delta W_t, \tag{3.11}$$

where Δf is considered as changes in the derivative price f within the small time period of Δt.

Since the Wiener process behind the stochastic process for the variable and its function is similar, the same uncertainty ΔW_t affects both S and f. Therefore, the portfolio that consists of one underlying and derivative can be established in a way that the Wiener process is eliminated. The establishment of such a portfolio is illustrated clearly by Hull (2012, p. 309-310). Driven by this, the equation (3.10) can be now given as follows:

$$\left(\frac{\partial f}{\partial t} + \frac{1}{2}\frac{\partial^2 f}{\partial S^2}\sigma^2 S^2\right)\Delta t = r\left(f - \frac{\partial f}{\partial S}S\right)\Delta t \tag{3.12}$$

aiming to

$$\frac{\partial f}{\partial t} + rS\frac{\partial f}{\partial S} + \frac{1}{2}\sigma^2 S^2\frac{\partial^2 f}{\partial S^2} = rf. \tag{3.13}$$

The equation (3.13) above is called the Black-Scholes differential equation representing one of the most essential findings based on Black and Scholes's (1973) study. Note that the equation (3.13) can be solved in many different ways, but usually it is applied to provide a closed-form solution for option prices. When the equation is solved, it leads to a certain partial derivative equation depending on the used boundary conditions. Boundary conditions are commonly applied to define an upper and lower limit for the acceptable

price of the derivative. The used boundary conditions may vary extensively due to the type of the derivative. Widely used boundary conditions for European-style call and put options are described below:

$$f_{call} = max\left(S_T - K, 0\right) \tag{3.14}$$

and

$$f_{put} = max\left(K - S_T, 0\right), \tag{3.15}$$

where T refers to the maturity time of the option. Moreover, S_T represents the asset price when t = T and K implies the strike price of the option.

As highlighted by Hull (2012, p. 313), one of the most remarkable solutions to the equation (3.13) is known as the Black-Scholes formulas to establish the prices for the European-style call and put options. Those can be given as follows:

$$C_t = S_0 N\left(d_1\right) - Ke^{-rT} N\left(d_2\right) \tag{3.16}$$

and

$$P_t = Ke^{-rT} N\left(-d_2\right) - S_0 N\left(-d_1\right), \tag{3.17}$$

where

$$d_1 = \frac{ln\left(S_0/K\right) + \left(r + \sigma^2/2\right)T}{\sigma\sqrt{T}} \tag{3.18}$$

$$d_2 = \frac{ln\left(S_0/K\right) + \left(r - \sigma^2/2\right)T}{\sigma\sqrt{T}} = d_1 - \sigma\sqrt{T}, \tag{3.19}$$

in which C_t and P_t represent the prices of the call and put options. While S_0 refers to the initial stock price (at time zero), σ is the volatility of the stock price, K and T are the strike price and maturity time of the option and r refers to the constant risk-free rate. On top of that, $N(x)$ represents the cumulative probability distribution function for a standard normal distribution.

Even though the BS model has been widely appreciated, it includes some illogical assumptions, which is one of the reasons why the model has been faced with some criticism about its accuracy and functionality (Teneng, 2011). As stated by Boyle and Mc-

Dougall (2019, p. 85-86), the BS theorem supposes that the underlying asset prices are log-normally distributed, and thus the prices cannot include jumps, which brings about a very controversial and unrealistic situation compared to the normal behaviour of the asset prices. Moreover, the model assumes that the volatility is constant, although the literature provides several deviant findings on this subject (e.g. Heston, 1993; Kienitz and Wetterau, 2013, p. 54).

On top of that, the Geometric Brownian motion itself has faced some negative discussion (Teneng, 2011). Since the Black-Scholes model supposes the asset prices are described by the random walk and the prices are log-normally distributed, there cannot occur any correlation between the asset prices. However, there actually has been observed a correlation between the prices driven by the fact that stock prices are determined by several social and economic factors which are correlated with each other as noted by Teneng (2011).

3.1.2 Heston model

Even though some asset pricing models assume that the volatility is constant, various studies have proven that the volatility development of the underlying asset indicates considerable variability. Hence, it is somewhat logical to consider non-constant volatility for hedging purposes and for evaluating the fair value of derivatives. These considerations have accelerated the development of stochastic volatility-oriented asset pricing models where the non-constant volatility, along the asset price, is also modelled as a stochastic process. (Kienitz and Wetterau, 2013, p. 54)

Heston (1993) introduced a stochastic volatility model along with a closed price solution for a European-style call option in a situation where the underlying asset price and its volatility correlate with each other. In the Heston model volatility evolves stochastically over time and it complies with a mean reverting process suggesting the volatility will eventually revert to the long-term mean value. By following Heston (1993), the diffusion equation for the asset price of S at time t can be described the following way:

$$dS_t = \mu S_t dt + \sqrt{v_t} S_t dW_t^1. \tag{3.20}$$

In comparison with the BS model the volatility is also assumed to follow a stochastic process. This is known as the variance process and is usually referred to as the square-root-process based on Feller (1951) and Cox et al. (1985). The variance of v can be defined as follows:

$$dv_t = \kappa(\theta - v_t)dt + \eta\sqrt{v_t} dW_t^2, \tag{3.21}$$

where κ represents the mean reversion speed of variance, θ is the long-term variance and η implies the non-stochastic volatility of the variance process known as the volatility of volatility. On top of that, W_t^1 and W_t^2 refer to the correlated Wiener processes with correlation $\rho > 0$. This relationship can be given as follows:

$$Cov(dW_t^1, dW_t^2) = \rho dt. \tag{3.22}$$

As highlighted by e.g. Mikhailov and Nögel (2004), there exists a condition for the variance process referred to as a Feller constraint. The purpose of the constraint is to ensure that the variance process will not reach zero. The Feller constraint can be described as follows:

$$2\kappa\theta \geq \eta^2. \tag{3.23}$$

However, applying the Feller constraint in connection with the Heston model has provoked a critical discussion in the literature and many practitioners actually do not fully comply with the constraint (e.g. Albrecher et al., 2007). Often the violation of the Feller constraint is required to ensure a better fit with the market data especially for derivatives with a long maturity.

In a similar fashion with the BS model, the Heston process need to be defined under the risk-free probability measure. By following Fiorentini et al. (2002) the Heston model under the risk-neutral probability measure can be described as follows:

$$dS_t = rS_t dt + \sqrt{v_t} S_t dW_t^{*1} \tag{3.24}$$

$$dv_t = \kappa^*(\theta - v_t)dt + \eta\sqrt{v_t} dW_t^{*2} \tag{3.25}$$

$$Cov(dW_t^{*1}, dW_t^{*2}) = \rho dt, \tag{3.26}$$

where κ and θ are replaced with risk-adjusted factors in the following manner: κ^* = $\kappa + \lambda_H$ and θ^* = $\kappa\theta$ / $(\kappa + \lambda_H)$. As noted by Fiorentini et al. (2002), λ_H refers to the market price of volatility that is needed to distinguish the physical probability measure from the risk neutral one.

In a similar manner with the BS model, the Heston model can be also adjusted into a more usable form by applying Itô's lemma. By following Heston (1993), the price of the

asset $U = (S, v, t)$ can be given through the following partial equation:

$$\frac{1}{2}vS^2\frac{\partial^2 U}{\partial S^2}+\rho\eta vS\frac{\partial^2 U}{\partial S\partial v}+\frac{1}{2}\eta^2 v\frac{\partial^2 U}{\partial v^2}+rS\frac{\partial U}{\partial S}+\{\kappa[\theta-v(t)]-\lambda_H v\}\frac{\partial U}{\partial v}-rU+\frac{\partial U}{\partial t}=0. \tag{3.27}$$

As highlighted by Heston (1993), a European call option with the maturity time of T and strike price K satisfies the above equation (3.27) through the following boundary conditions:

$$\begin{aligned} U(S,v,t) &= max(0, S-K) \\ U(0,v,t) &= 0 \\ \frac{\partial U}{\partial S}(\infty,v,t) &= 1 \\ rS\frac{\partial U}{\partial S}(S,0,t)+\kappa\theta\frac{\partial U}{\partial v}(S,0,t)-rU(S,0,t)+U_t(S,0,t) &= 0 \\ U(S,\infty,t) &= S. \end{aligned} \tag{3.28}$$

The price of a European call option C can be obtained through the solution for the partial differential equation (3.27). We can observe many similarities with the BS model, where the corresponding PDE was solved by using the equation (3.16). Instead of using the direct method, Heston (1993) provided a solution for the equation (3.27) by applying a characteristic function. The solution can be defined as follows:

$$C(S_0, K, v_0, t, T) = SP_1 - Ke^{-(r-q)(T-t)}P_2, \tag{3.29}$$

where P_1 and P_2 are two risk-neutralized probabilities. P_1 refers to the delta of the European call option whereas P_2 implies the conditional risk neutral probability that the underlying asset price of S will be greater than the strike price of K at the maturity of T. Within this illustrative equation $T - t$ refers to the time to maturity.

Based on Heston (1993) and Mikhailov and Nögel (2004) both probabilities of P_1 and P_2 can be derived numerically from the following integral equation for j = 1,2 as follows:

$$P_j = \frac{1}{2}+\frac{1}{\pi}\int_0^\infty Re\left[\frac{e^{-i\phi lnK}\varphi_j(S_0, v_0, t, T, \phi)}{i\phi}\right]d\phi. \tag{3.30}$$

The numerically solution for the risk-neutralized probabilities of P_1 and P_2 are introduced in more detail in Section 3.3. As proposed by Heston (1993), the solution for the charac-

teristic functions of φ_1 as well as φ_2 can be given:

$$\varphi_j(S_0, v_0, \tau, \phi) = e^{C_j(\tau;\phi)+D_j(\tau;\phi)v_o+i\phi S_0}, \tag{3.31}$$

where $\tau = T - t$. Furthermore, the solutions for the unknown functions of $C_j(\tau;\phi)$ and $D_j(\tau;\phi)$ can be referred to as follows:

$$C_j(\tau;\phi) = (r-q)\phi i\tau + \frac{\kappa\theta}{\eta^2}\left\{(b_j - \rho\eta\phi i + d)\tau - 2ln\left[\frac{1-ge^{d\tau}}{1-g}\right]\right\} \tag{3.32}$$

and

$$D_j(\tau;\phi) = \frac{b_j - \rho\eta\phi i + d}{\eta^2}\left[\frac{1-e^{d\tau}}{1-ge^{d\tau}}\right] \tag{3.33}$$

including

$$g = \frac{b_j - \rho\eta\phi i + d}{b_j - \rho\eta\phi i - d} \tag{3.34}$$

$$d = \sqrt{(\rho\eta\phi i - b_j)^2 - \eta^2(2u_j\phi i - \phi^2}, \tag{3.35}$$

where $u_1 = \frac{1}{2}$, $u_2 = -\frac{1}{2}$, $a = \kappa\theta$, $b_1 = \kappa + \lambda_H - \rho\eta$ and $b_2 = \kappa + \lambda_H$.

3.2 Jump diffusion models

Even though the diffusion models are rather widely used in option pricing, they do not necessarily describe the movements of the underlying asset in a realistic way. As noted by Kienitz and Wetterau (2013, p. 93) the diffusion models are not capable of modelling the impacts of rare events such as defaults, crashes or credit events. More familiarly, such rare events are referred to as jumps. In all its simplicity, a jump can occur if an essential piece of information about a publicly listed company becomes available causing an unexpected change in the company's stock price (Cížek et al., 2005, p. 184).

Over the years, there have been proposed several pricing models that allow the occurrence of jumps. Within this thesis, we only deal with the diffusion models that have been extended to capture discontinuous movements. These models are known as the jump diffusion models consisting of the diffusion and jumping parts. As highlighted by Kienitz and Wetterau (2013, p. 93), the jump diffusion models are usually conducted by adding an uncorrelated compound Poisson process to the diffusion part.

A Poisson process can be considered as a certain stochastic process for a series of

discrete events as noted by Iacus (2011, p. 109). It is recognized by its feature where the exact timing of discrete events occurs randomly, but in turn, the average time between the events is known. Furthermore, each event is independent and thus the previous event does not impact on the current event. In general, there are several definitions for the Poisson process in the literature, but according to Iacus (2011, p. 109), the process can be illustrated as follows:

$$N_t = N(t) = N([0, t]), \tag{3.36}$$

where N_t is a value of the process up to time t. The number of events between certain time t is modelled as $\Delta N_t = N_{t+\Delta t} - N_t$ where $t + \Delta t$ is a small time-interval. The Poisson process N_t follows a Poisson distribution if the following condition is satisfied:

$$P(N_t = k) = e^{-\lambda t} \frac{(\lambda t)^k}{k!}, k = 0, 1, 2..., \tag{3.37}$$

where $\lambda > 0$ can be seen as the expected number of events during the time-interval. In general, the Poisson distribution gives a probability of observing k events within a given time-period. Driven by the Poisson process, the occurrences of jumps are included in the pricing models through a compound Poisson process. The compound Poisson process can be defined as follows:

$$X_t = \sum_{i=1}^{N_t} Y_{\tau_i}, \tag{3.38}$$

where N_t is the Poisson process and Y_{τ_i} refers to the jumps at random times τ_i, which are independent and identically distributed random variables. (Iacus, 2011, p. 109-111)

3.2.1 Merton model

Merton (1976) introduced an early stage jump diffusion model which has proven to be an important part of the further development of asset pricing models. The Merton model is briefly illustrated below due to its strong relationship with the Bates model that has been applied in the empirical part of this thesis.

To cope with sudden jumps in the price of the underlying asset, Merton (1976) suggested a model which allows the discontinuous movements of asset prices. In all its simplicity, the Merton model is an extended version of the Black-Scholes model by integrating the jump term to the equation (3.8). By following Cížek et al. (2005, p. 184), the asset price

dynamic can be given as follows:

$$dS_t = \mu S_t dt + \sigma S_t dW_t + dZ_t, \tag{3.39}$$

where Z_t refers to the compound Poisson process with the log-normally distributed jump sizes. The jumps comply with the Poisson process N_t with the jump intensity of λ. The log-normally distributed jump sizes are identically distributed random variables, independent of both the Wiener process and the Poisson process.

Corresponding with the Heston model and Black-Scholes model, the Merton model should be adjusted with a risk neutral probability. As noted by Cížek et al. (2005, p. 185), the Merton model can be referred to as an incomplete model, and thus there exists many different ways to adopt the risk neutral probability. Driven by Merton (1976), the authors of Cížek et al. (2005, p. 185) proposed only to adjust the drift μ of the Wiener process and keep the other conditions unchanged. Thus, the price dynamic can be modelled in the following manner:

$$S_t = S_0 e^{\mu_M t + \sigma W_t + \sum_{i=1}^{N_t} Y_i}, \tag{3.40}$$

where $\mu_M = \mu - \sigma^2 - \lambda e^{\left(\mu_j + \frac{\delta^2}{2}\right) - 1}$. In this illustrative example, the log-jump sizes are denoted by Y_i with the mean of μ_j and variance δ^2. Compared to the traditional Black-Scholes model, the included jump components assign more weight to the tails of the return distribution as concluded by Cížek et al. (2005, p. 185).

Based on Kienitz and Wetterau (2013, p. 96), the pricing of European options can be completed either through the closed form solution of the characteristic function or by using similar equations as presented with the Black-Scholes model (3.16 - 3.19). The option pricing through the Merton model has been left out from this thesis. However, more information about this subject can be found in Merton (1976), Kienitz and Wetterau (2013, p. 96) and Cížek et al. (2005, p. 185).

3.2.2 Bates model

The Merton model and the Heston model were reconciled into the new model by Bates (1996). The Bates model is practically an extension of the Heston model with an additional jump diffusion part in the price process. In a similar fashion with the Heston model, the Bates model also assumes that the variance process is stochastic. Moreover, when the model complies with the stochastic volatility, it is able to define smile and skew effects of implied volatility. The dynamics of the Bates model have been briefly illustrated below by following Bates (1996). Note that there might appear some minor denotation differ-

ences compared to the Merton model introduced last section. Based on Bates (1996), the dynamics can be given as follows:

$$dS_t = (\mu - \lambda\overline{k})S_t dt + \sqrt{v_t}S_t dW_t^1 + kdq \tag{3.41}$$

$$dv_t = \kappa(\theta - v_t)dt + \eta\sqrt{v_t}dW_t^2 \tag{3.42}$$

$$Cov(dW_t^1, dW_t^2) = \rho dt \tag{3.43}$$

$$Prob(dq = 1) = \lambda dt. \tag{3.44}$$

These equations are mostly in line with the Heston model equations (3.20 - 3.22) with the exception of the equation (3.41) including a jump diffusion part. The jump diffusion term dq refers to a compound Poisson process with intensity λ and log normally distributed jump sizes being independent of dW_t^1 and dW_t^2. The equation of $ln(1+k)$ illustrates the jump sizes being normally distributed and thus it can be described as $ln(1+k) \sim N\left(ln(1+\overline{k}) - \frac{1}{2}\delta^2, \delta^2\right)$, where $\overline{k}$ refers to the mean jump size.

Similar to the previously introduced models, the dynamics above should be defined under a risk neutral probability measure to satisfy the risk neutral world. Based on Bates (1996), the model dynamics with risk neutral probabilities can be given as follows:

$$dS_t = (r - \lambda^*\overline{k}^*)S_t dt + \sqrt{v_t}S_t dW_t^{*1} + k^* dq^* \tag{3.45}$$

$$dv_t = \kappa^*(\theta^* - v_t)dt + \eta\sqrt{v_t}dW_t^{*2} \tag{3.46}$$

$$Cov(dW_t^{*1}, dW_t^{*2}) = \rho dt \tag{3.47}$$

$$Prob(dq^* = 1) = \lambda^* dt \tag{3.48}$$

$$ln(1+k^*) \sim N\left(ln(1+\overline{k}^*) - \frac{1}{2}\delta^2, \delta^2\right), \tag{3.49}$$

where λ^* and $\overline{k}^*$ refer to adjustments for the market price of jump risk as follows $\lambda^* =$

$\lambda(1+\overline{k})$ and $\overline{k}^* = \overline{k} + \frac{\delta^2}{1+\overline{k}}$. Moreover, the risk-adjusted factors of κ^* and θ^* comply with the same conditions as defined with the risk adjusted Heston process.

When it comes to the price of a European call option, the price can be calculated in the same way as was done with the Heston model. Driven by similarities with the Heston model, the equations (3.29) and (3.30) are applicable also for the Bates model. However, the difference in the pricing results is attributable to the different characteristic functions. According to Bates (1996) and Sepp (2003), the characteristic function for the Bates model can be determined in accordance with the following procedure:

$$\varphi_j(S_0, v_0, \tau, \phi) = e^{C_j(\tau;\phi)+D_j(\tau;\phi)v_o+i\phi S_0+\tau\Lambda(\phi)}, \tag{3.50}$$

where τ = $T - t$. The solutions for the unknown functions of $C_j(\tau;\phi)$ and $D_j(\tau;\phi)$ correspond to equations of (3.32 - 3.35). In turn, $\Lambda(\phi)$ can be described as follows:

$$\Lambda(\phi) = e^{(\overline{k}+I_j\delta^2/2)i\phi-\delta^2\phi^2/2+I_j(\overline{k}+\delta^2/2)} - 1 - (i\phi + I_j)(e^{\overline{k}+\delta^2/2} - 1), \tag{3.51}$$

where $I_j = u_j + \frac{1}{2}$ and $u_1 = \frac{1}{2}, u_2 = -\frac{1}{2}$.

3.3 Option pricing with the fast Fourier transform

In the previous sections, Heston (1993) and Bates (1996) asset pricing models and their characteristic functions were explained. As mentioned previously, to define the price for a European call option, equation (3.30) requires a numerical solution for the derivation of P_1 and P_2. The solution can be derived, for example, by applying an approach based on the Fourier transform or alternatively based on the fast Fourier transform (FFT) which has been applied in this thesis. The option pricing through the FFT has been introduced by Carr and Madan (1999).

As highlighted by Cížek et al. (2005, p. 188), the main idea of the FFT method is to define an analytical expression for the Fourier transform of the option price and to calculate the price through the Fourier inversion. The authors further noted that the FFT provides a significant speed advantage making it a really practical tool in option pricing. However, it should be noted that the FFT method assumes that the characteristic function of the pricing model should be known and defined analytically before. The basic concept of the FFT has been briefly illustrated below by following Carr and Madan (1999).

At first, the analytic expressions for the Fourier transform of a certain option price have been defined. Suppose that the log of the strike price is denoted by k. Thus, $C_T(k)$ refers to the expected value of a call option with the strike price of $exp(k)$ and the maturity time of T. In addition, s_T implies the log price and the risk-neutral density of s_T is referred to

as $q_T(s)$. Within this illustrative example, the characteristic function of this density can be given by:

$$\phi_T(u) \equiv \int_{-\infty}^{\infty} e^{ius} q_T(s) ds. \tag{3.52}$$

Furthermore, the initial call value of $C_T(k)$ can be written in the following manner:

$$C_T(k) \equiv \int_{k}^{\infty} e^{-rT}(e^s - e^k) q_T(s) ds. \tag{3.53}$$

As can be seen from above, the presented function is not square-integrable since $C_T(k)$ tends to s_0 and moreover k tends to $-\infty$. To achieve a square-integrable function, the modified call price of $c_T(k)$ is applied. This can be presented as follows:

$$c_T(k) \equiv exp(\alpha k) C_T(k). \tag{3.54}$$

The modified call price can be recognized as square-integrable for a suitable range of $\alpha > 0$. As a result of this, the Fourier transform of $c_T(k)$ can be now determined as follows:

$$\psi_T(v) = \int_{-\infty}^{\infty} e^{ivk} c_T(k) dk. \tag{3.55}$$

After that, the analytical expression for the Fourier transform of $\psi_T(v)$ in terms of the characteristic function of ϕ_T can be defined through the following procedure:

$$C_T(k) = \frac{exp(-\alpha k)}{2\pi} \int_{-\infty}^{\infty} e^{-ivk} \psi_T(v) dv = \frac{exp(-\alpha k)}{\pi} \int_{0}^{\infty} e^{-ivk} \psi(v) dv, \tag{3.56}$$

where the statement for the Fourier transform of $\psi_T(v)$ is given as follows:

$$\psi_T(v) = \frac{e^{-rT} \phi_T(v - (\alpha^2 + 1)i)}{\alpha^2 + \alpha - v^2 + i(2\alpha + 1)v}. \tag{3.57}$$

Now, when the analytical expression for the Fourier transform has been defined above, the call option price in terms of $\psi_T(v)$ can be derived through the Fourier inversion. At first, let's provide a numerical solution for the integration (3.56) as an application of the following sum equation for k = 1,...,N:

$$w(k) = \sum_{j=1}^{N} e^{-i\frac{2\pi}{N}(j-1)(k-1)} x(j), \tag{3.58}$$

where N is typically considered as N^2. The authors Carr and Madan (1999) especially noted that the FFT offers a powerful algorithm to compute the given sum equation (3.58). The speed advantage of the FFT approach is driven by the algorithm's ability to reduce the number of multiplications in the required N summations. Next, $C_T(k)$ based on the equation (3.56) can be described through the sum equation (3.58) as follows:

$$C_T(k) \approx \frac{exp(-\alpha k)}{\pi} \sum_{j=1}^{N} e^{-iv_j k} \psi_T(v_j)\eta, \tag{3.59}$$

where $v_j = \eta(j-1)$, $j = 0, ..., N-1$, and $\eta > 0$ refers to the distance between the points of integration grid.

Carr and Madan (1999) were mainly interested in at-the-money call option values appearing in the situation where k is near to zero. While the FFT returns N values of k they suggested a regular spacing size of λ, and thus their values for k can be described as $k_u = -b + \lambda(u-1)$ for u = 1,...,N. This in turn indicates that the log strike levels varying from $-b$ to b where $b = \frac{N\lambda}{2}$. Furthermore, by substituting the equation of $k_u = -b + \lambda(u-1)$ into equation (3.59) and considering previously introduced $v_j = \eta(j-1)$, the European call option price can be written as:

$$C_T(k_u) \approx \frac{exp(-\alpha k_u)}{\pi} \sum_{j=1}^{N} e^{-i\lambda\eta(j-1)(u-1)} e^{ibv_j} \psi_T(v_j)\eta. \tag{3.60}$$

When comparing the equation above (3.60) with the summation (3.58), the variable of $\lambda\eta$ equals $\frac{2\pi}{N}$. Carr and Madan (1999) suggested to use comparatively large values for η to end up with a more accurate integration result. For that purpose, the authors decided to apply Simpson's rule into their summation. Finally, the conclusive equation for the European call option price can be written as follows:

$$C(k_u) = \frac{exp(-\alpha k_u)}{\pi} \sum_{j=1}^{N} e^{-i\frac{2\pi}{N}(j-1)(u-1)} e^{ibv_j} \psi_T(v_j) \frac{\eta}{3}(3 + (-1)^j - \delta_{j-1}). \tag{3.61}$$

Regardless of the easy implementation of Carr and Madan's (1999) approach, there exists several alternative approaches for pricing options by applying Fourier methods. Many of these have similarities with the Carr and Madan (1999) method and, for example, Cont and Tankov (2004, p. 366) proposed an alternative solution for the equation (3.54) by considering the modified time value of the options as follows:

$$c_T(k) = C_T(k) - max(1 - e^{k-rT}, 0). \tag{3.62}$$

Instead of using an analytical approach (i.e Fourier transform methods), the option prices can be obtained also through simulation techniques. Such a well-known simulation approach is referred to as the Monte Carlo simulation. The Monte Carlo simulation is applied to model the probability of varying outcomes for a certain process occurring randomly. It is a rather widely used approach in option pricing as instead of focusing on only the European-style options, it is also capable of modelling a wider class of derivatives such as exotic and path dependent options as noted by Cížek et al. (2005, p. 197) and Cont and Tankov (2004, p. 179).

3.4 Implied volatility and implied volatility surfaces

A common way to define the volatility of the stock price of σ is to acquire some historical asset pricing data and calculate its standard deviation to come up with an estimate of the volatility. Another way is to define so-called implied volatility which refers to a forward-looking expectation of volatility. It deviates from historical volatility in a way that it is not concluded from known past returns of a security but rather it is based on the market's forecast of a likely movement in the security's price. (Boyle and McDougall, 2019, p. 89-91)

In other words, implied volatilities correspond to the volatilities implied by option prices observed in the market. In many cases implied volatility is parallel with the Black-Scholes model which offers a convenient way to calculate the implied volatility by reverting the process and using the option prices derived from somewhere else. That relationship has been exemplified clearly by Zulfiqar and Gulzar (2021) as follows:

$$C_{market} = S_0 N\left(d_1\right) - K e^{-rT} N\left(d_2\right), \tag{3.63}$$

where

$$d_1 = \frac{ln\left(S_0/K\right) + \left(r + \widehat{\sigma^2}/2\right) T}{\widehat{\sigma}\sqrt{T}} \tag{3.64}$$

$$d_2 = d_1 - \widehat{\sigma}\sqrt{T}, \tag{3.65}$$

where $\widehat{\sigma}$ refers to the implied volatility that forces the market observed price to be equal to the model call price.

It should be noted that implied volatility can be also obtained by applying other asset pricing models, and thus the outcome is heavily dependent on the used model and its assumptions. Moreover, there are many studies in the literature trying to define implied

volatility with improved precision and accuracy. For example, Yan and Jianhui (2016) and S. Liu et al. (2019) focus on describing implied volatility by using Neural Networks. However, unless otherwise stated, in this thesis implied volatility is deducted through the Black-Scholes model following the approach presented above.

As noted before, implied volatility provides useful information about the market's estimate of possible movements in a security's price. Apart from that, implied volatility has often been used to understand better the option dynamic by observing the behaviour of implied volatility as a function of the strike price or moneyness. According to Hull (2012, p. 409) this relationship for a particular maturity is often referred to as an implied volatility smile.

Empirical studies have shown that typically the shape of the function between implied volatility and strike price resembles a semicircle (smile) or an oblique semicircle (skew). For a given expiration, options whose strike price deviates significantly from the underlying asset's price contribute to higher prices for derivatives, and thus for implied volatilities. (Boyle and McDougall, 2019, p. 127-129) Hence by graphing implied volatilities in terms of strike prices for a particular maturity, it generates a smile or skew rather than the expected flat surface, as would be seen in the Black-Scholes model (Cont and Da Fonseca, 2002). As a matter of fact, since the BS model is not capable of modelling implied volatility smiles (Boyle and McDougall, 2019, p. 127), it brings out another limitation of the BS model which questions its applicability. Other limitations and drawbacks were discussed in more detail in Section 3.1.1.

The relationship between implied volatility and option dynamics has usually been defined through an implied volatility surface. Implied volatility surfaces are commonly illustrated as a three-dimensional plot of maturity, strike (or moneyness) and implied volatility. By following Cont and Da Fonseca's (2002) research, the implied volatility surface at time t can be given as a function below with the outputs of $\mathbb{R}_+$:

$$\widehat{\sigma}_t : (K, T) \rightarrow \widehat{\sigma}_t(K, T), \tag{3.66}$$

where $\widehat{\sigma}_t(K, T)$ refers to the implied volatility with a strike price K and maturity time T. Typically, the formed surface is also evaluated from a smile or skew perspective.

Volatility surfaces also work the other way around. According to Cont and Da Fonseca (2002), specifying the implied volatility surface at a given date provides an approximation of prices for all (vanilla) options at that date. In other words, the volatility surface can be applied to estimate the derivative's unknown implied volatility as well as the monetary price for the missing maturity-strike combinations. However, extrapolated figures should always be used with caution. This is also supported by Rouah (2015, p. 40) who points out that the extrapolation of the implied volatility surface beyond the known and observable strikes may lead to arbitrary values.

3.5 Selection of the models

According to Cao and Celik's (2021) article, regardless of the popularity of cryptocurrency derivatives, there is neither an accurate valuation framework to capture the complicated behaviour of cryptocurrencies nor a means to establish the fair value of cryptocurrency derivatives in a consistent fashion. This is also supported by Jalan et al. (2021) who argue that it is not a simple task to summarize the valuation dynamics of bitcoin options driven by the extreme volatile and uncertain behaviour, since the common principles of efficient market and investor sentiments may not apply to cryptocurrency markets.

Despite the possible challenges encountered in bitcoin option pricing, there are some studies on the topic. To mention a few of them, for example, Cretarola et al. (2020) established a closed pricing formula for European-style bitcoin derivatives and Cao and Celik (2021) proposed an analytical valuation model for bitcoin options that is based on the modified Merton jump diffusion model (Section 3.2.1). Furthermore, Hou et al. (2020) provided a way of pricing bitcoin options through the stochastic volatility with a correlated jump model (known as SVCJ) (Duffie et al., 2000) and the stochastic volatility model with a non-linearity structure (known as BR model) as suggested by Bandi and Renò (2016).

As mentioned before, the Heston model and the Bates model have been chosen to be used within this thesis. Even though previous studies have given us valuable insights on the valuation dynamics relating to bitcoin option pricing, we emphasized the simplicity of the model over its capabilities to capture the uncertain behaviour of cryptocurrencies. Since the main focus of this thesis relates to model calibrations, the most complex models are excluded from the review in order to make the calibration efficient and fast enough.

Note that a model calibration process within the cryptocurrency context is still a relatively understudied topic in the literature. Madan et al.'s (2019) research can be considered as one of the few studies focusing purely on the model calibration from a cryptocurrency perspective, thus it has been referred to several times in a later stage of the thesis. Also, Teng and Härdle (2022) provided some insights about the SVCJ model calibration to bitcoin options. However, since their study has been performed by following the inverse options principles, it is not so relevant for the purpose of this thesis as mentioned in the beginning of this chapter.

Driven by the absence of the jump diffusion parameters for the Heston model, it will be interesting to observe how the final calibration results deviate between the Heston and Bates models. Especially considering that the occurrence of jumps in the crypto markets are rather typical as observed by Hou et al. (2020). All in all, since the fundamentals of both models have been widely explored among practitioners, the literature is considered to provide enough reliable information to evaluate and analyse the obtained results in a coherent fashion.

4. MODEL CALIBRATION

This chapter introduces the main features of a model calibration process, the Nelder-Mead algorithm (Nelder and Mead, 1965) as well as standard errors and stabilities of model parameters. Finally, the illustrative effects of changing parameters will be explained.

4.1 Model calibration process

Model calibration is a widely recognized procedure in statistical modelling which is neither restricted to any particular type of model nor to a specific industry. Model calibration can thus be encountered in numerous contexts. Judd and Judd (2011, p. 252) define the model calibration process as finding a unique set of model parameters that provides a sufficient description of the system behaviour, and can be achieved by confronting model predictions with actual measurements performed on the system or model.

From a financial perspective, a model calibration refers to a process of fitting an asset pricing model to market data by optimizing the model parameters in a way that those model prices replicate as closely as possible with the market prices, write Büchel et al. (2022). The model calibration process has had a remarkable role in the development of advanced pricing models, as newly structured finance solutions and more complicated derivatives have constantly been granted in the markets. The more accurate the calibration results are, the more valid the predictability of a pricing model is, which in the best case can lead to a high-value tool from a portfolio and risk management perspective.

The calibration process commonly starts with the identification of a loss function to be minimized. Rouah (2015, p. 116-118) highlighted in his book that there are a lot of different ways to establish a loss function, but fairly often they fall into two main categories. The first category focuses on those that minimize the error between quoted and model prices, whereas the second category minimizes the error between quoted and model implied volatilities. Typically these errors are determined as the squared, absolute or relative difference between the quoted and the model prices or volatilities. According to Escobar and Gschnaidtner (2016), the applied loss function contributes a lot to the calibration outcomes.

By following Rouah (2015, p. 116-117), widely used loss functions to define the mean squared errors (MSE) between the market quotes and model prices or model implied volatilities can be given in the following manner:

$$MSE = \frac{1}{N}\sum_{T,K}(C_{TK} - C_{TK}^{\Theta})^2 \tag{4.1}$$

$$IV - MSE = \frac{1}{N}\sum_{T,K}(IV_{TK} - IV_{TK}^{\Theta})^2, \tag{4.2}$$

where C_{TK} and IV_{TK} refer to quoted prices and quoted implied volatilities with a given maturity time T and strike K. Hence, C_{TK}^{Θ} and IV_{TK}^{Θ} imply model prices and model implied volatilities. Apart from that, N represents the number of quotes. The application of the MSE loss function assigns relatively more weight on expensive options, such as options within in-the-money position and those with a long maturity. Instead, the IV-MSE loss function allocates approximately equal weight to options regardless of the moneyness level since the calculated implied volatilities end up at a similar magnitude compared to the quoted implied volatilities.

Sometimes MSE-based loss functions are replaced by root mean squared error loss functions (RMSE) as they can be directly interpreted in terms of measurement units. In the literature, you can come across different definitions, but practically RMSE is computed by taking the square root of MSE. Kienitz and Wetterau (2013, p. 435), have illustrated the RMSE-based loss function the following way:

$$RMSE = \frac{1}{\sqrt{N}}\sqrt{\sum_{T,K}(C_{TK} - C_{TK}^{\Theta})^2}, \tag{4.3}$$

where C_{TK} and C_{TK}^{Θ} refer to quoted and model prices for each maturity-strike combination in the same way as in the equation (4.1).

Quoted market prices applied in the calibration usually depend on data availability, and of course, the purpose of which the calibration procedure has been designed for. In general, quoted prices tend to correspond to certain types of mid prices, such as the average between the available bid and ask prices. However, sometimes the required quoted prices are not available at all, or they can be obtained just for a given maturity-strike combination. This offers a possibility to perform a calibration through the quoted implied volatilities instead of the quoted prices. In fact, the applicability of the model is typically evaluated by comparing model and quoted implied volatilities because options are usually quoted in terms of implied volatility as argued by Rouah (2015, p. 117).

In terms of a decent calibration outcome, the liquidity of the applied options should be

considered carefully since illiquid options may lead to distorted calibration results (Sayer and Wenzel, 2015). Liquidity of a financial instrument refers to how easily an instrument can be traded without impacting its current market price (Verousis et al., 2016). Therefore, liquid options can be sold or bought more likely at a fair market price. In this thesis the model calibrations have been carried out by applying vanilla options, which usually reflect relatively good liquidity in a general manner. However, this is not guaranteed in the cryptocurrency context since crypto markets have not proven to be as liquid as more established asset classes according to Alexander, Heck, et al. (2022).

The lack of liquidity between the options is usually covered by assigning different weights to the loss function. Based on Sayer and Wenzel's (2015) article, the weights are in many occasions set in a way that they emphasize the liquidity of the instrument by giving relatively more weight to frequently traded instruments. However, there is not one right way as to which weighting should be chosen and as stated by Rouah (2015, p. 117) the choice of the weights is usually very subjective. As an example can be taken Christoffersen et al. (2009) who utilized a widely known approach called BS-vega where the squared BS-vega has been used as weight. By following Rouah (2015, p. 117), the BS-vega loss function can be presented as follows:

$$Vega - MSE = \frac{1}{N} \sum_{T,K} \frac{(C_{TK} - C_{TK}^{\Theta})^2}{BSvega_{TK}^2}, \tag{4.4}$$

where BS-vega represents the sensitivity of the option price in terms of the quoted implied volatility IV_{TK}.

Although the importance of loss functions has been studied widely in the literature, such as in papers of Bams et al. (2009) and Escobar and Gschnaidtner (2016), there is no simple consensus as to which loss function should be chosen (Rouah, 2015, p. 117). Within this thesis the IV-MSE loss function (4.2) has been selected. Because this thesis also focuses on what kind of implied volatility surfaces European-style bitcoin call options develop, the IV-MSE loss function serves the purpose best.

When the loss function has been identified, the next phase focuses on finding a reasonable optimization algorithm to minimize the loss function. Similar to the loss function selection, there is no a simple consensus as to which optimization algorithm or method should be chosen. Pachamanova and Fabozzi (2010, p. 144) summarize in their book that the increase in computational power during the past 20 years has resulted in relatively systematic and accurate algorithms and practical software for solving optimization problems of many kinds.

To end up with satisfied optimization results, the optimization problem may be constrained for a specific purpose according to the true nature of the optimization problem, param-

eters or loss function. These kinds of optimizations are referred to as constrained optimization problems. In turn, optimization problems with no constrains can be referred to as unconstrained problems. (Pachamanova and Fabozzi, 2010, p. 144) In this thesis, the optimization problem is constrained as the pricing models to be calibrated impose some constrains on their parameters. Sometimes the optimization can also be constrained through a penalty term as proposed by Sayer and Wenzel (2015). The penalty term is commonly defined as the difference between the calibrated parameters and some prearranged parameters and its main purpose is to stabilize the calibration (Sayer and Wenzel, 2015). On the other hand, it can manipulate the calibration results if the behaviour of the underlying asset tends to be rather unstable.

A function can have many minimum points, in which case the global minimum is the "most" minimum point for the function, whereas the local minimum represents the other minimum points. With respect to the most complex loss functions, the shape of the function can be unknown, and thus it may be a bit risky to apply a local optimization algorithm. However, finding a global optimal solution can be rather difficult and time consuming. (Pachamanova and Fabozzi, 2010, p. 147-148) Although the most classical optimization algorithms are only capable of finding local optima, in practice they tend to work reasonably well for such a function without too many minimum points. It should be noted that the local optimizer requires proper initial values as highlighted by Escobar and Gschnaidtner (2016). In this thesis the Nelder-Mead optimization algorithm has been applied. Please refer to Section 4.2 for details.

Even if the calibrated asset pricing model can perfectly match the obtained results to the market data, it does not necessarily mean that the calibrated parameters are reliable or that the selected model can capture an asset's real movements in the long run. As stated by Escobar and Gschnaidtner (2016), the obtained parameters rarely represent so-called true parameters that would immediately be suitable in future option pricing. The calibration process always involves some degree of risk, and as Escobar and Gschnaidtner (2016) remarked, most of the risk factors driving overall calibration results can be divided into model risks and calibration risks.

Based on Yu et al. (2018), model risk represents a source of risk being attributable to incorrect models and overall model misuse. In other words, even though the calibration is carried out as correctly and rationally as possible, the wrong model or its misuse can lead to unreliable outcomes. This is also referred to as model uncertainty (Cont, 2006). On the contrary, calibration risk includes all other calibration aspects, such as choosing an optimization algorithm, error function and initial parameters. These risk factors should be always critically evaluated before the obtained true parameters are used in future option pricing. (Escobar and Gschnaidtner, 2016)

4.2 Nelder-Mead optimization algorithm

In this thesis, the Nelder-Mead optimization algorithm has been applied. It is a widely known numerical method to find the minimum or maximum point of a multidimensional objective function and it was originally illustrated by Nelder and Mead (1965).

The algorithm follows a direct search method without using any derivative-related approach. In other words, the functionality of the method is attributable to whether the new value leads to a better result than the previous value. (Lagarias et al., 1998) As described by Nelder and Mead (1965), the algorithm applies a simplex consisting of $n + 1$ vertices as starting values within n dimensions. Below is provided a simple example of how the algorithm works by following Lagarias et al.'s (1998) article. The main steps of the method are (i) order, (ii) reflect, (iii) expand, (iv) contract and (v) shrink. These are illustrated in Figure 4.1.

Let's consider a simple function of $g(x, y)$ to be minimized. Since our function is a two-dimensional function, a simplex of a triangle including 3 vertices is needed. At first, three points have to be selected of a, b and c in 2D to build up our simplex and evaluate the value of the function g at those three points and **order** them according to the function's value. Since this is only an illustrative example, it can be assumed that the points are arranged as follows:

$$g(a) < g(b) < g(c). \tag{4.5}$$

After this, the worst point of c is **reflected** through the centroid of other points of a and b and thus we obtain a reflected point of d. On top of that, the value of the function g is evaluated at point d in the same way as before. If the outcome of the function at the reflected point $g(d)$ performs better than $g(b)$ but worse than $g(a)$, the previously considered worst point of c is replaced with d.

However, if $g(d)$ provides a better outcome in comparison to both $g(a)$ and $g(b)$, the iteration continues to an extension phase. As a result of this, the reflected point of d is **expanded** even further from the centroid becoming an expanded point of e. After the expansion, if the outcome of the function at the expanded point $g(e)$ is even better compared to the reflected point of $g(d)$, the previously considered worst point of c will be replaced with e instead of the reflected point d. However, if the expanded point does not lead to better outcomes, the worst point of c is replaced with d as originally intended.

Moreover, if neither the reflected phase nor the expanded phase are satisfied, it is rather useless to try to enhance the simplex through the reflected point d since the point itself performs worse than the starting points of a and b. Therefore, the worst point of c is **contracted** into two points of c_a and c_b along the reflected line. The point c_a is called an

inside contracted point between c and d, whereas c_b is called an outside contracted point between c and d. Similar to previous phases, the value of the function g is evaluated at points c_a and c_b. If either of these contracted points lead to better results than $g(b)$, the worst point of c is then replaced with a better performing point of c_a or c_b.

Finally, if neither of the contracted points of c_a nor c_b lead to better outcomes than b, then the simplex is **shrunk** towards the best performing point of a. This is well illustrated in Figure 4.1 where the points c and b are replaced by c_{new} and b_{new}.

The outcomes of a local optimization algorithm depend strongly on the initial parameters as noted by Escobar and Gschnaidtner (2016). The choice of initial parameters is illustrated in more detail within Section 5.5.

4.3 Standard error and stability of the parameters

Parameters obtained through a calibration process can be quite unique for a given underlying asset at a given time even if the parameter-specific restrictions are properly considered. Especially, if market conditions fluctuate widely during the selected review period, the true parameters may experience rather heavy variation as argued by Escobar and Gschnaidtner (2016). Thus it may be difficult to estimate what the true parameters should look like for absolute terms. We note that there are several approaches to estimate parameters' behaviour in the literature, but in this thesis, we compose an understanding of how relevant and valid the true parameters are by observing their (i) standard errors and (ii) stability over time, as suggested by Kienitz and Wetterau (2013, p. 511).

Parameters' standard errors imply how sensitive the calibration results are to changes in the model parameters. Furthermore, this can also be considered rather useful from a statistical analysis perspective since standard errors are needed when calculating t-values. A brief description of how standard errors of parameters are calculated in this thesis is presented below.

First of all, let us define the function f obtained as a result of the calibrations as follows:

$$f = \frac{1}{N} \sum_i (\hat{y}(i) - y(i, \Theta))^2, \tag{4.6}$$

where $\hat{y}(i)$ refers to the quoted implied volatilities and $y(i, \Theta)$ refers accordingly to the model implied volatilities for the parameters of Θ. Note that Θ can represent either Heston or Bates parameters depending on whether the standard errors are calculated with the Heston model or Bates model. The model implied volatilities are defined as $g_i = y(i, \Theta)$ where g_i refers to the i_{th} element of the model output.

Moreover, since the standard errors for each parameter are derived through a covariance

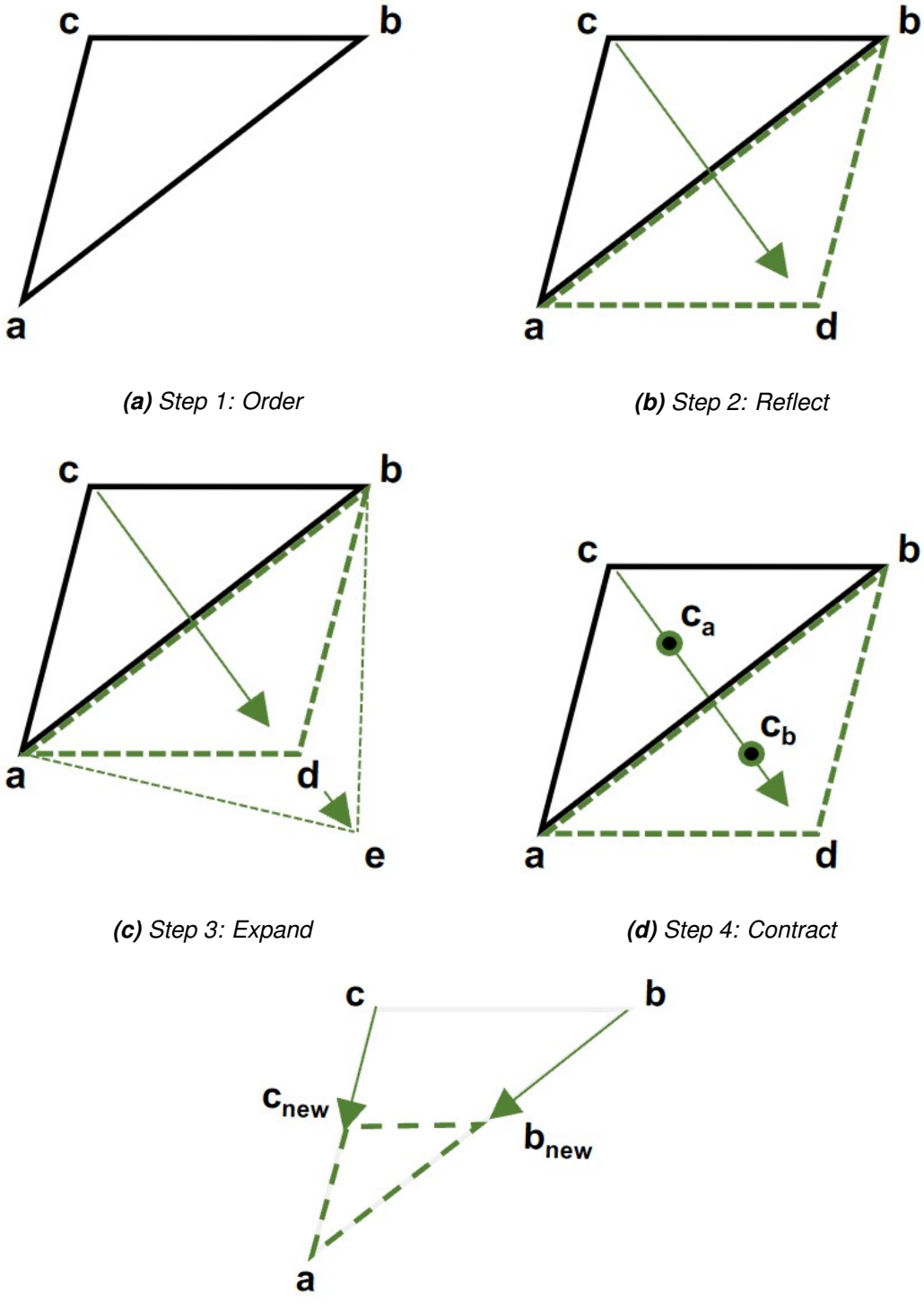

(a) *Step 1: Order*

(b) *Step 2: Reflect*

(c) *Step 3: Expand*

(d) *Step 4: Contract*

(e) *Step 5: Shrink*

Figure 4.1. *An illustrative example of the Nelder-Mead method with a two-dimensional function (Lagarias et al., 1998).*

matrix, let's define the covariance matrix Σ in following manner:

$$\Sigma = \hat{\sigma}^2 (J'J)^{-1}, \tag{4.7}$$

where $\hat{\sigma}^2$ equals to $\frac{f}{N-p}$ in which N means the number of options whereas p refers to the number of parameters. At same time, J refers to the Jacobian matrix (often referred to as Jacobian) representing a matrix that collects all first-order partial derivatives of a function with multiple variables. Within this case, the entry of J_{ij} for the Jacobian matrix can be descried as $J_{ij} = \frac{\partial g_i}{\partial \Theta_j}$ where Θ_j means the j_{th} element in a set of model parameters (either Heston or Bates). By following Simon and Blume (1994, p. 325), this can be illustrated explicitly as follows:

$$J = \begin{bmatrix} \frac{\partial g_1}{\partial \Theta_1} & \cdots & \frac{\partial g_1}{\partial \Theta_n} \\ \vdots & \ddots & \vdots \\ \frac{\partial g_m}{\partial \Theta_1} & \cdots & \frac{\partial g_m}{\partial \Theta_n} \end{bmatrix}. \tag{4.8}$$

Finally, the standard error for each parameter i can be defined by the following equation:

$$SEi = \sqrt{Diag(\Sigma_{ii})}. \tag{4.9}$$

Conclusively, the smaller the standard error, the more significant is the impact on the calibration results. This helps us to estimate how reliably we can use the obtained parameters.

When it comes to the stability, Kienitz and Wetterau (2013, p. 511) introduce a couple of different measures to estimate the parameters stability over time. In this thesis, a relative mean measure was used focusing on an average of parameters' relative daily changes. This is given as follows:

$$M_R = \frac{1}{(N-1)} \sum_{i=2}^{N} \frac{\Theta_{t_i} - \Theta_{t_i - 1}}{\Theta_{t_i - 1}}, \tag{4.10}$$

where Θ_{t_i} denotes a certain model parameter calibrated at time t_i.

4.4 Qualitative effects of changing parameters

Before proceeding with empirical considerations, this section has a brief look at what the changes in parameters actually mean. This part illustrates how changing the model parameters affects the shape of the implied volatility smile and skew by following Cížek

et al. (2005, p. 171-173). As highlighted in Section 3.4, the implied volatility smile refers to the implied volatility as a function of the strike price or moneyness for a given maturity.

At first, the effects of changing the volatility of volatility of η is evaluated. By adjusting η being equal to zero, the variance turns into a deterministic process, and thus volatility does not include any smile resulting in a flat smile curve. On the contrary, by increasing the volatility of volatility it accelerates the convexity of the smile impacting on its steepness. When it comes to the other volatility-basis parameter, initial variance v_0, it produces a somewhat different impact on the volatility smile. Changes in v_0 concern the height of the smile more than the shape.

With regards to the long-term variance θ, the effects of changing the parameter (ceteris paribus) are somewhat similar in comparison with those observed by changing the initial variance v_0. In other words, the changes in θ also impact on the height of the smile rather than the shape. Associated with the mean reversion speed of variance κ, the changes are conversely related to the steepness of the smile affecting more the ATM part than the high ends of the curve. On top of that, increasing the mean reversion simultaneously lifts the centre.

While looking at the influence of the correlation ρ, the uncorrelated relationship ($\rho = 0$) provides a fit that reminds of an almost symmetric smile with a centre point near ATM. Consequently, by changing ρ the degree of symmetry changes. In other words, ρ defines the skewness of the volatility smile.

According to Kienitz and Wetterau (2013, p. 103), by combining the Heston model with a jump diffusion part, the jump diffusion parameters impact more on the short end of the implied volatility smile. They also argue that increases in the mean jump size of $\overline{k}$ shift the skew to the right, whereas decreases push the whole skew more to the left. On the contrary, the changes in the standard error of the jump size δ impact on the height of the smile. Practically, increasing δ lifts the smile and the whole implied volatility surface upwards, and vice versa. When it comes to the jump intensity λ, the changes result in a nearly equivalent shift of the whole surface.

Overall, model parameters can have similar effects on the implied volatility smile and thus, from an efficient calibration perspective, some parameters can be thought to be fixed and only calibrate the remaining parameters. As proposed by Cížek et al. (2005, p. 171-173), the effects driven by the increases in the mean reversion speed of variance κ are usually compensated by consequently higher values for the volatility of volatility η. A similar type of relationship can be observed with the initial and long-term variance of v_0 and θ. In some cases it appears to be reasonable to select the fixed v_0 in advance and only let the long-term variance differ. Moreover, fixing certain parameters has proven to be useful in the testing phase before the actual calibrations as demonstrated by Kienitz and Wetterau (2013, p. 509) in their calibrations.

5. RESEARCH METHODOLOGY AND DATA

This chapter gives a brief introduction to the research process used in this thesis. In addition, the applied dataset, the main assumptions of the empirical part and the considerations about the reliability and validity of the results will be elaborated here.

5.1 Research process

The purpose of this master's thesis is to conduct a calibration of asset pricing models to the European-style call options, which use the bitcoin as an underlying asset. Furthermore, this thesis aims to cover the following research questions keeping the main focus on the latter one. Firstly, what kind of implied volatility surfaces do European-style bitcoin call options develop, and how do those change across the review period. Secondly, what kind of parameters and mean squared errors are obtained when the Heston and Bates asset pricing models are calibrated against quoted implied volatility surfaces, and how do those parameters and mean squared errors develop throughout the review period.

This thesis uses a quantitative research design by acquiring, processing as well as analysing a numerical data set. According to Saunders et al. (2019, p. 175-176), quantitative research is often associated with generating or using numerical data, and in many cases quantitative research can be seen as a deductive approach where data is collected and analysed to test, for example, a theory or hypothesis.

A research process was defined as a part of the background work. The research process consisted of several smaller steps which together helped to build a clear guideline for this thesis. At first, it was determined what the goals of the study are. Connected to that, research questions were defined. Secondly, empirical data applied in the thesis was acquired and processed to be in a more usable form. Thirdly, all necessary programming was implemented and tested for building the implied volatility surfaces and model calibrations. After this the implied volatility surfaces within the review period were established and the Heston and Bates models were calibrated. Finally, the empirical results were gathered and analysed.

5.2 Data

The empirical part of this thesis is based on data acquired from the Deribit cryptocurrency derivative exchange through the application programming interface (API). Deribit is a Netherland-based trading platform founded in 2016, making it one of the oldest exchanges for trading cryptocurrency derivatives. Deribit is a widely used exchange whose listed products include amongst others bitcoin (BTC) and ethereum (ETC) options and futures.

According to Hoang and Baur (2020), Deribit is the first platform in the world offering BTC options although other kind of BTC derivatives, such as futures and perpetuals contracts, had been traded on other exchanges before the foundation of Deribit (e.g. BitMEX that was founded in 2014). Moreover, they noted that Deribit can be currently considered one of the largest crypto derivative exchanges in terms of daily trading volumes.

Bitcoin options traded by Deribit are European-style and hence they can be only exercised at the expiry. Furthermore, option contrasts can be traded 24/7 and they expire on each Friday at 08:00 UTC. Based on discussions with Deribit's support department they do not provide historical data for their instruments. However, it is possible to acquire a snapshot of quotes on any traded instruments through Deribit's API. Such a snapshot provides a wide range of information including e.g. bid and ask prices, volumes, open interests as well as underlying asset prices.

Starting on the 30thof September 2021 at 22:53:45 UTC the applied BTC option data (snapshot) was downloaded within approximately every 60 minutes until the 31st of October 2021 at 21:47:23 UTC. One snapshot included several option contracts involving both European-style call and put options. Each option contract was defined as a certain underlying-maturity-strike-option type combination (e.g. BTC-2JUL21-42000-C). It should be noted that there were some inconsistent snapshots and timestamps without any data. However, these had no effect in terms of the final result of the empirical part.

5.3 Data processing

While the BTC data was acquired, it was at the same time pre-processed including the following steps: (i) data was transformed into a mat file, (ii) underlying-maturity-strike-option type strings were separated from each other, (iii) creation timestamps as well as maturities were converted from the unix timestamps to UTCs and (iv) irrelevant information was excluded. Driven by the pre-processing phase, the remaining variables can be seen in Table 5.1 below.

After pre-processing was completed, the option prices (ask, bid and mark prices) were converted to US dollars since the downloaded option prices were initially denominated

Table 5.1. *Variables involved in the BTC data after the pre-processing phase.*

Variable	Description
AskPrice	The ask price of the BTC option
BidPrice	The bid price of the BTC option
MarkPrice	The current value of the BTC option as calculated by Deribit risk management
Maturity	The expiration date and time of the BTC option
OptionType	Describing whether the BTC option is put or call
TimeStamp	The creation timestamp for the data snapshot
TimeToMaturity	The length of time until the option contract expires
UnderlyingPrice	The underlying price of bitcoin

in BTCs. The conversion was performed by applying the underlying BTC prices as they were denominated in US dollars. It should be noted that the underlying price might vary between different option contracts in the same timestamp. The prices for each option are determined through the order book process, while the actual time stamps for each option are determined according to buy and sell orders that investors have made for a particular security. Therefore, the creation timestamp for observations (different options in the timestamps) deviates from the actual timestamps leading to different underlying prices.

The downloaded BTC data from Deribit did not contain risk-free rates which are needed in implied volatility calculations as well as option pricing. For this thesis, risk-free rates are based on short-term US government debt obligations (Treasury Bills, T-Bills). Since the United Sates is an AAA-rated country and the underlying and option prices have been converted into US dollars, applying Treasury Bills as a proxy for risk-free rates can be considered reasonable.

The applied Treasury Bill data is based on the Federal Reserve Economic Data (FRED) offering a wide range of data series and tools. The downloaded Treasury Bill data involved daily spot rates across the review period from the 30^{th} of September to the 31^{st} of October 2021 with a maturity of (i) 4 weeks, (ii) 3 months, (iii) 6 months as well as (iv) 12 months. Based on those maturities, the corresponding risk-free rate was defined for each BTC option contract in terms of the option's maturity date. Furthermore, all the snapshots within the same daily timestamp used the corresponding daily Treasury Bill spot rate.

If the time to maturity of the option was less than 30 days, a Treasury Bill rate with a maturity of one month was used as a risk-free rate. When the option's time to maturity was between 30 days and 90 days, the applied Treasury Bill rate was derived through linear interpolation between maturities of 4 weeks and 3 months. Similar linear interpolation was used for the options with time to maturities between 90 days and 180 days as well as

between 180 days and 360 days. For those options with a maturity being more than 360 days, a Treasury Bill rate of one year was applied.

The acquired BTC data involved also European-style put options. Since both implied volatility surfaces and model calibrations in this thesis are based on European-style call options, each of the put option prices was converted into call option prices by applying a put-call parity - equation. Put-call parity describes the relationship between put and call options and was introduced by Stoll (1969). The theory states that the price of a put option indicates the fair value for a corresponding call option if that call option has the same strike price, underlying price and maturity. This theory applies both ways and in practice it defines the three-sided connection between puts, calls as well as underlying assets. The general form of the equation is given below:

$$C_t + Ke^{-rT} = P_t + S_t, \tag{5.1}$$

where C_t and P_t refer to prices for a call option and put option. Moreover, S_t represents an underlying asset price, r is a risk-free rate while K and T model option's strike price and time to maturity, respectively.

After converting put options to call options, the options were revised for possible arbitrages. Similar to Section 3.1.1, some boundary conditions were considered to limit the acceptable price of the derivative. Firstly, the equation of $C_t < S_t$ was applied, because the European-style call option to buy a share of security cannot be more valuable than the fair value of the share. Secondly, the equation of $C_t > max(S_t - Ke^{-rT}, 0)$ was applied to verify that if there are no dividends prior to expiration, the European-style call price should never fall below zero.

While each option was reviewed for possible arbitrages, the implied volatilities based on market data were calculated through the Black-Scholes model. As referred to in Section 3.4 the Black-Scholes model offers a convenient way to calculate the implied volatility by using the option prices derived from somewhere else. In this thesis, MarkPrice - variables were applied as a proxy for those BTC option prices quoted in the market. The implied volatilities based on market data were calculated by solving $\hat{\sigma}$ using equations (3.63 - 3.65).

As a final part of the data processing, the BTC data was filtered by removing all the options that (i) led to arbitrage or (ii) ended up in either an infinity value or NaN value after converting the monetary call price into the implied volatility. Apart from those, some maturity and moneyness restrictions were applied to improve comparability between the different data snapshots. As a result, one snapshot typically consisted of approximately 300 to 400 different BTC option contracts with maturities ranging from less than one month up to almost one year.

5.4 Implied volatility surface derivation

The construction of IV-surfaces is based on the processed data introduced in Section 5.3. Since the data was acquired approximately every 60 minutes, there were quite many snapshots in total. Thus the implied volatility surfaces in this thesis were established by applying a snapshot every 24 hours as far as it was possible. As already mentioned, there were some inconsistent snapshots and timestamps during the review period, but those did not have a major impact on the final results.

Moreover, it should be noted that the number of BTC options in the snapshots may deviate across the review period. This is mainly driven by the expiration of some options and may cause issues from a comparability perspective. Therefore the IV-surfaces were established with a constant grid (maturity and moneyness).

In the constant grid, maturity remained between one month and ten months, whereas the lower limit of moneyness (S/K) was 0.5 and the upper limit was 2.0. However, if a data snapshot did not meet the selected maturity and moneyness restrictions, the constant grid was adapted according to the snapshot. In these cases, the new constant grid was based on the lowest and highest maturity and moneyness of the processed data for a given snapshot.

IV-surfaces in this thesis were based on interpolation. For that purpose, a query grid (query points) was created at first, based on the constant grid restrictions (selected maturity and moneyness) for a given snapshot. After this, Matlab's ready-to-use Volatility-Surface.m code library was used in which the processed data of (i) time to maturity (ii) moneyness and (iii) implied volatility was adjusted to a more usable form. To end up with a more consistent and interpretable volatility surface, implied volatility was also smoothed by applying Gaussian kernel smoothing. Finally, an implied volatility surface for a given snapshot was interpolated over a defined grid using linear interpolation.

5.5 Model calibration derivation

Similar to the implied volatility surface derivation, the same processed data and same range of snapshots (every 24 hours) were applied as a background for the model calibrations. As referred previously, the Heston and Bates asset pricing models are calibrated by using implied volatilities of the BTC options instead of monetary market prices. Therefore, the IV-based loss function (4.2) was used in this thesis. None of weights was used in the loss function since the IV-MSE allocates approximately equal weight to options regardless of the moneyness level. Note that if NaN values existed when calculating the model implied volatilities, they were converted to be equal to 1.

With regards to the optimization, the Nelder-Mead algorithm was selected to be applied

in this thesis (please refer to Section 4.2). In Matlab, a fminsearch - function represents the Nelder-Mead approach attempting to find a minimum x of the specified function using derivative-free method. Since the fminsearch - function is capable of finding a minimum of a multivariable function, it was considered suitable for calibrating the Heston and Bates asset pricing models.

Given that in some cases optimization can be a rather long and unclear process, some settings and restrictions were set for the Nelder-Mead algorithm. However, it should be noted that there is not a simple consensus as to which of the optimization settings and restrictions should be used. With regards to this thesis, the applied settings are given in Table 5.2 below.

Table 5.2. *Optimization settings and restrictions.*

Setting	**Description**
MaxFunEvals = 1600	Maximum number of function evaluations allowed
MaxIter = 1600	Maximum number of iterations allowed
TolFun = 1e-4	Termination tolerance on the function value
TolX = 1e-4	Termination tolerance on x
FunValCheck = 'on'	Check whether objective function values are valid. 'on' displays an error when the objective function returns a value that is complex or NaN

As noted previously, the Heston and Bates models were calibrated to BTC snapshot data at 24-hour intervals. For calculating option prices, both pricing models were based on Kienitz and Wetterau's (2012) ready-to-use programming libraries. The authors gave a numerical solution for the equation (3.30) through the fast Fourier transform method based on Carr and Madan's (1999) approach (see Section 3.3 for details).

With regards to optimization, it should be noted that the solutions of the local optimization algorithm depend strongly on the initial parameters. As stated by Rouah (2015, p. 123) and Escobar and Gschnaidtner (2016), the selected initial parameters should not be too far from the true parameters obtained as a result of the calibration. For the first calibration rounds of both models, eight sets of different parameters were randomly generated. The parameters that provided the smallest value for the loss function (IV-MSE) were chosen as starting values for the first calibration rounds. Furthermore, from the second calibration onwards, previously calibrated parameters were used as starting values for the next calibration. Even though parameters can have similar effects to a volatility smile, each parameter was included in the calibration instead of fixing some parameters and only calibrating the remaining parameters as suggested by Cížek et al. (2005, p. 171-173).

The applied restrictions of calibrated parameters were mostly the same for both models, with the exception of the jump diffusion parameters that were only characteristic for the

Bates model. The models themselves imposed some constrains on those parameters, an example of which is the correlation ρ that is only allowed to vary between -1 and 1. Moreover, the volatility and variance related parameters such as (i) long-term variance θ, (ii) volatility of volatility η, (iii) initial variance v_0 as well as (iv) standard deviation of the jump size δ were limited to be positive. Since the standard deviation is the square root of variance, it is always non-negative. With respect to other parameters, several test calibrations were performed to get some guidelines for the restrictions. Based on the testing phase it was noticed that the jump intensity λ varies quite a lot, so no upper limit was set for that parameter. The restrictions applied in this thesis can be found in Table 5.3 below.

Table 5.3. *Parameter restrictions.*

Parameter	**Lower boundary**	**Upper boundary**
Mean reversion speed of variance, κ	0.5	35
Long-term variance, θ	0.01^2	2.5
Volatility of volatility, η	0.01^2	25
Correlation, ρ	-1	1
Initial variance, v_0	0.01^2	2
Mean jump size, $\overline{k}$	-1.5	1.5
Standard deviation of the jump size, δ	0	1
Jump intensity, λ	0	∞

It should be noted that the Feller constraint (3.23) was excluded from the analysis to improve the fit between the model prices and the market quotes especially for BTC options with a long maturity. Background of the Feller constraint was presented in more detail in Section 3.1.2.

In association with the model calibrations, the stability of each parameter was assessed by using the relative mean measure (4.10). Furthermore, the standard errors for each parameter were calculated in order to be able to analyse better how sensitive the results obtained from calibrations are to changes in model parameters. The standard error calculations were performed through the Jacobian matrix which has been introduced in more detail in Section 4.3. It should be noted that if the Jacobian matrix produced NaN values, they were converted to 0. Since each of the calibrated values of the jump diffusion parameter δ were so close to zero, the singular values had to be modified to ensure the Jacobian matrix did not turn into a singular matrix. Therefore the calculated standard errors of δ did not represent valid values.

5.6 Reliability and validity of the results

One considerable part of the research process is to assess the quality of the results. There are several measures of qualities in a quantitative study, but in this thesis the focus was set on reliability and validity.

Both of those measures have multiple definitions and extensions in literature, for instance, Saunders et al. (2019, p. 213) have described reliability and validity as follows. Reliability represents the replication and consistency of the research. In other words, whether the results can be replicated under the same conditions. In turn, validity represents the appropriateness of the measures applied, accuracy of the analysis of the results as well as generalisability of the findings. Meaning whether the received results really represent what they are intended to measure.

In this thesis, reliability was reflected by complying with a consistent and efficient programming road map for obtaining the results. The repeatability of the results was improved by making the programming as dynamic as possible without including unnecessary manual inputs. However, when it came to the provided calibrations the optimization algorithm had an essential role in terms of the results obtained, and thus even a small change in parameter restrictions or optimization settings could have led to inconsistent results. Since both models were calibrated applying BTC data from a certain time frame, the calibrations would lead to different results if the applied data set was based on another time frame.

From a validity perspective, some testing calibrations were performed by applying randomly selected option combinations (not more than 10 options) to ensure that the optimization was working correctly. Additionally, validity aspects were considered also within the implied volatility surfaces. By following the observations from the literature introduced in Section 4.4, it was verified whether changes in the Heston and Bates's parameters impact the IV-surfaces in the way they were supposed to.

All in all the study consisted of a constant effort to ensure the quality of the results. As mentioned previously the results were rather sensitive to changes in the main assumptions. Therefore, instead of blindly relying on the obtained findings, it is recommended to perform calibrations and IV-surface derivations again if there were to arise any changes in the applied data set or used optimizations restrictions and settings.

6. EMPIRICAL RESULTS AND DISCUSSION

This chapter includes the empirical results and discussion of this thesis which are presented in two main steps. The first part focuses on the implied volatility surfaces whereas the second part considers the model calibrations of the Heston and Bates models.

6.1 Implied volatility surfaces

As mentioned in Section 5.4, the implied volatility surfaces in this empirical part were created by taking a snapshot at 24-hour intervals. When plotting these IV-surfaces the log moneyness ($log\frac{S}{K}$) was applied instead of normal moneyness ($\frac{S}{K}$). This means that at-the-money options (ATM) equal to 0 and conclusively in-the-money (ITM) and out-the-money options (OTM) represent positive and negative values. The implied volatility surface based on the BTC option quotes of the first data snapshot on the 30th of September 2021 is given in Figure 6.1.

When observing the plotted IV surface, the formed smile effect where the implied volatility increases when moneyness either decreases or increases, is clearly visible. This is mostly attributable to the general insight that ITM and OTM options cover additional risk driven by possible large movements in the underlying away from the ATM position. Corresponding to that increased risk, ITM and OTM options are typically priced higher as highlighted in Section 3.4.

The smile function achieves its minimum near the ATM, following general principles of the implied volatility surface modelling. The smile appears very clearly at short time to maturities, whereas it becomes more and more indefinite as time to maturity increases. In addition, a typical pattern for ITM options can be observed, where the implied volatility gradually decreases while time to maturity increases. These observations are supported by Fengler (2005, p. 30-32).

From a cryptocurrency perspective, the formed smile at short time to maturities also seems to be reasonable. In their study, Zulfiqar and Gulzar (2021) verified the existence of an implied volatility smile in bitcoin options and they argued that the smile is the deepest for options near expiry. They further concluded that short-term bitcoin options tend to provide higher volatility. This observation is in line with Alexander, Deng, et al. (2022) who

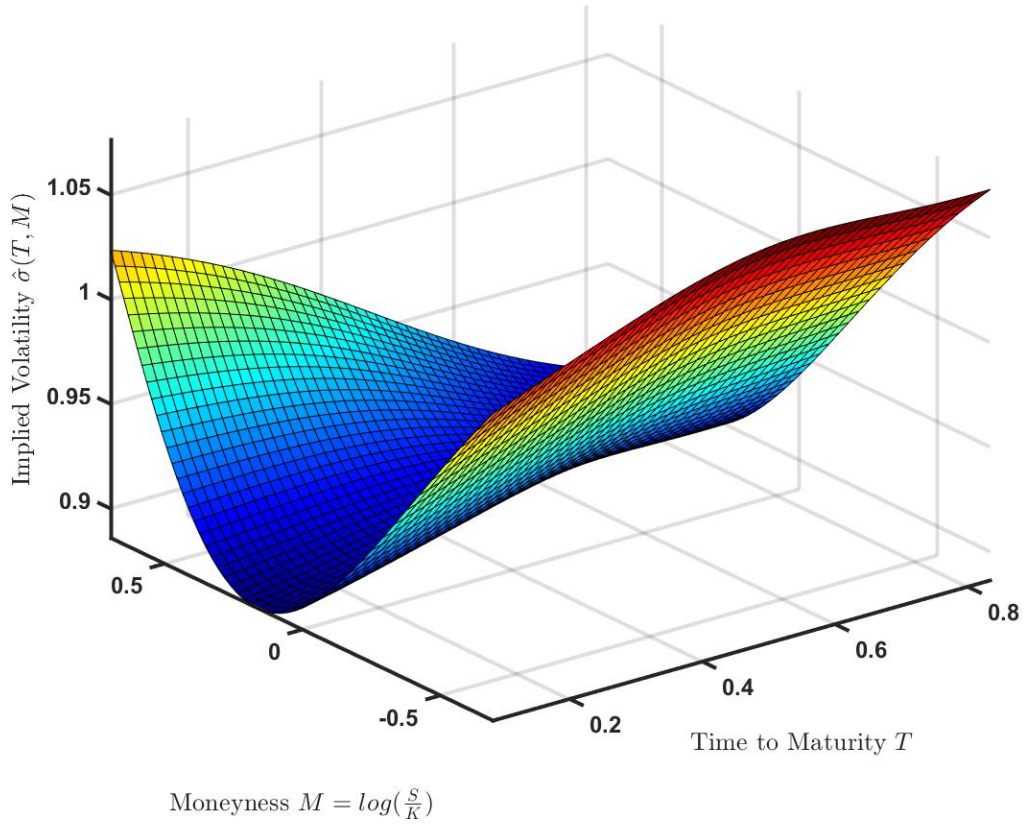

Figure 6.1. *Implied volatility surface based on BTC market data from the 30th of September 2021.*

argue that short-term options are traded more often in the bitcoin option market. Therefore, the short-term options have a greater market risk and hence they are more sensitive to volatility than long-term options. Relatively high demand for short-term bitcoin options can be partly explained by the crypto-option traders' willingness to hedge their positions or alternatively gain higher option premiums on BTC call and put options.

The established volatility smile with short time to maturities is also rather symmetric. Similar behaviour was also recognized by Alexander, Deng, et al. (2022) who summarized in their research that bitcoin options provide usually a more symmetric smile compared to the more typical "skew" shape for S&P 500 options. They noted that the slopes of implied volatility curves for S&P 500 options turn more negative if thoughts of a stock market crash become more topical. On the contrary, the negative left and positive right slopes of bitcoin options' smiles prove that both negative as well as positive price jumps are expected.

On a general level, the implied volatility across the applied grid appears to be relatively high. As mentioned before, implied volatility indicates the market's view about the underlying's potential moves without considering whether the underlying moves upwards or downwards. So roughly, on the 30th of September 2021 the market estimates that bitcoins

have a relatively high probability for large price movements in either direction. This seems reasonable by reflecting the historical performance and development of bitcoin.

The conducted implied volatility seems to fluctuate around 100%. Although it can be considered rather high for absolute terms, the level is still somewhat in line with the general consensus on the implied volatility of bitcoin options. Based on Alexander, Deng, et al.'s (2022) article, the ATM volatility of the bitcoin IV curve usually fluctuates around 100%, being at the same time very variable. The authors also noted that the bitcoin IV curve is much higher compared to the IV curves of S&P 500 options where the ATM volatility has been around 20% for a long time.

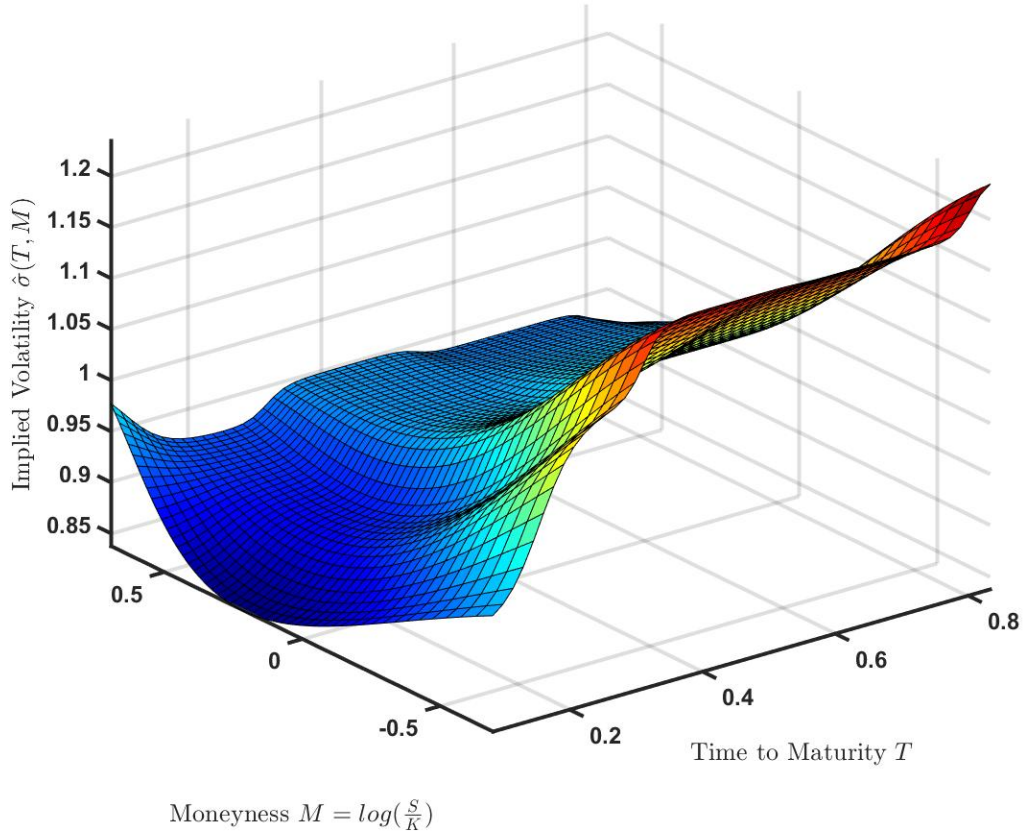

Figure 6.2. *Implied volatility surface based on BTC market data from the 22nd of October 2021.*

When the IV surfaces were formed over the review period, it was noticed that the plotted surfaces deviate quite a lot from each other. With respect to each surface, we can still observe a rather clear smile effect at short time to maturities. However, as timet to maturity increases, the surfaces become heavily forward skew shaped. The forward skew represents a specific volatility profile where OTM call options and ITM put options are priced at a higher implied volatility. However, according to Zulfiqar and Gulzar's (2021) study, this is not an unusual situation for bitcoin options. In their study, most of the conducted volatility smiles of the BTC options ended up in the forward skew shape. They further noted that

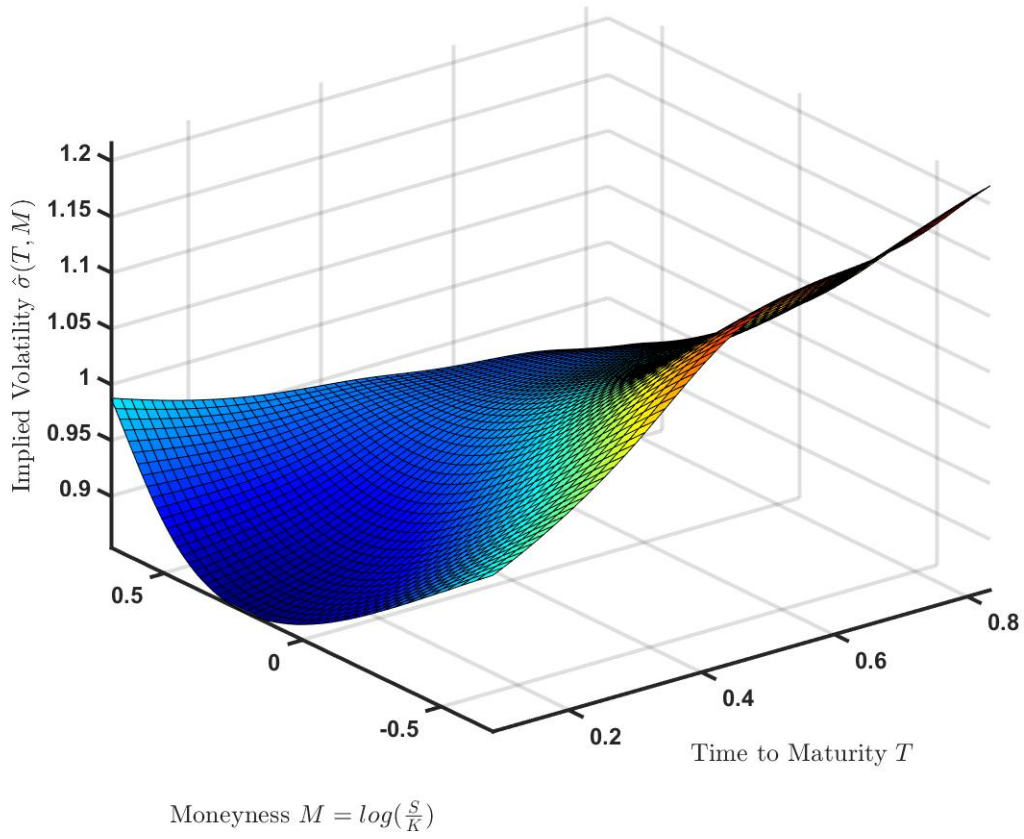

Figure 6.3. *Implied volatility surface based on BTC market data from the 31st of October 2021.*

this forward skewness observed in BTC options is driven by the increased demand for buying OTM calls to hedge bitcoin price risk. Similar observations were provided also by Hoang and Baur (2020) as part of their research on forecasting bitcoin volatility. The differences across the review period are illustrated in Figures 6.2 and 6.3, where the IV surfaces are based on snapshots from the middle and end of the review period. The previously mentioned forward volatility skew can be seen clearly from Figure 6.2.

There are several explanatory factors that drive the differences between the surfaces across the review period. On a general level, the changes in the formed surfaces can be partly explained by bitcoin's tendency to be just a really risky asset. General factors such as regulations, continuous media hype as well as just the irrational behaviour of investors can heavily accelerate the fluctuation of bitcoin's price. Consequently, this can change the shape of the surface considerably even within a short period of time. Bitcoin's strong price changes were also empathized by W. Zhang et al. (2021) and Alexander, Deng, et al. (2022) in their studies, where they stated that the fundamental value of bitcoin and the factors driving its price are still rather unclear and not widely acknowledged. Correspondingly, also Hou et al. (2020) highlighted the volatile price behaviour of bitcoin. They argued that BTC option prices are heavily driven by jumps causing changes in the

shape of the IV curves.

In addition, implied volatility surfaces can be strongly impacted by certain types of logical explanations such as the expiration of certain maturity-strike option combinations or new supply and demand conditions. Unexpected changes within supply or demand cause variation in the option price, and thus also in the implied volatility. This is supported, for example, by Fengler (2005, p. 44) who highlighted the contribution of supply and demand conditions to the shape of the smile. On top of that, also Bollen and Whaley's (2004) empirical results indicate that implied volatility is directly related to the options' demand and supply pressure. With respect to BTC options, net buying pressure and trading motives have been studied by Alexander, Deng, et al. (2022).

Alexander, Deng, et al. (2022) summarized that bitcoin option traders are generally less risk averse than, for example, more common S&P 500 options traders. Furthermore, they noted that the bitcoin option traders comply with volatility-motivated demand. When the traders are volatility-motivated, volatility shocks to the underlying asset leads to changes in traders' expectations towards volatility. In other words, volatility shocks would shift the option supply curves and consequently affect the implied volatility smile and surface.

6.2 Model calibrations

Similarly to the implied volatility surfaces, both models have been calibrated to BTC data from the 30th of September 2021 to the 31st of October 2021 by applying a data snapshot at 24-hour intervals. The used assumptions and settings related to the calibration process were presented in more detail within in 5.5.

In the big picture, the model calibrations for the Heston model went fairly smoothly while the calibrations for the Bates model were slightly more problematic. With the Bates model, the calibration process for each data snapshot took a comparatively long time and the deviation in some parameters were somewhat large and appeared to be unreasonable for absolute terms. Of course, it must be understood that the Bates model has three additional parameters compared to the Heston model bringing extra complexity to the table. To get a better overall picture, the IV-MSE development across the review period is presented in Figure 6.4.

When observing the IV-MSE development from Figure 6.4, it can clearly be seen that the IV-MSEs obtained as a result of the calibrations follow the same trend. While the IV-MSE for the Bates model increases, the IV-MSE provided by the Heston model increases accordingly, and vice versa. However, it can be noted that the changes were not so sensitive for the Bates model.

Furthermore, each calibration round for the Bates model resulted in a smaller mean squared error compared to the Heston model indicating that the Bates model allows for a

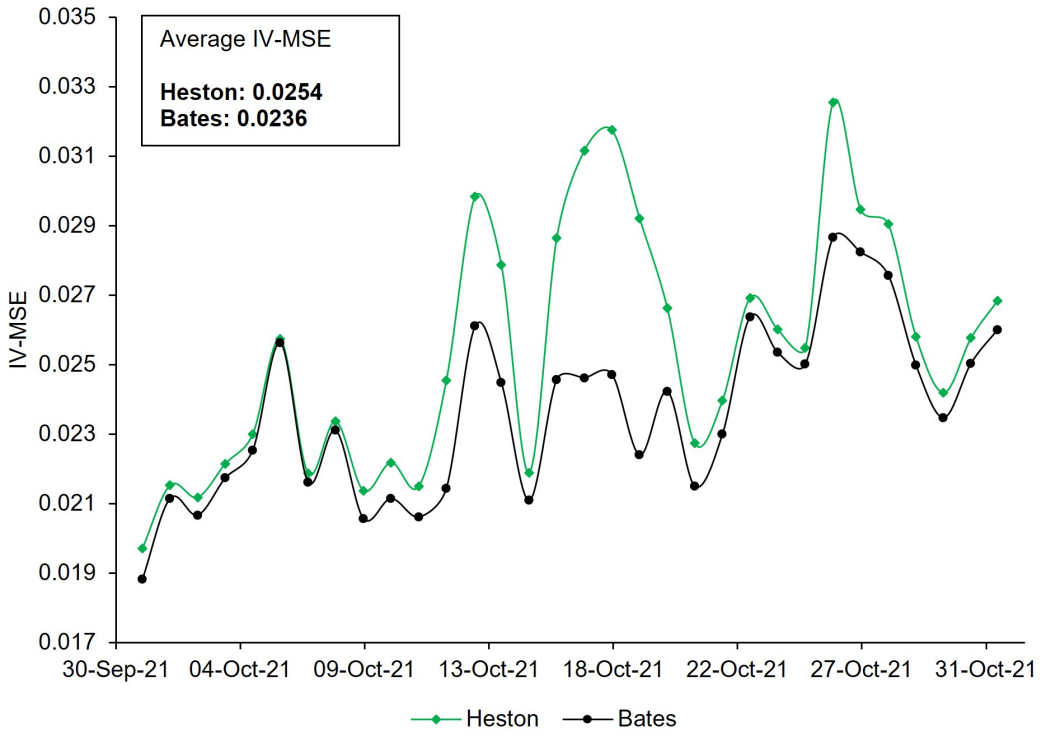

Figure 6.4. *Implied volatility mean squared errors for calibrating the Heston and Bates models to BTC option data from the 30th of September 2021 to the 31st of October 2021.*

better fit between the model and quoted implied volatilities without considering any other aspects, such as how appropriate the parameters actually were in terms of pricing. This is in line with Kienitz and Wetterau's (2013, p. 508) arguments that the additional jump parameters of the Bates model can be used to better fit the short end of the implied volatility surface. In other words, the processes involved in the Heston model are continuous and cannot move so steeply as argued by Sayer and Wenzel (2015). This relationship can be observed easily from Figure 6.5 where both models were calibrated to BTC options of the first data snapshot from the 30th of September 2021 (Figure 6.1).

Overall, both models still produced a relatively good fit for short-maturity options considering the evidence that such options typically represent high liquidity (Fengler, 2005, p. 20) and thus are likely to reflect market's fair value improving the calibration results (Büchel et al., 2022; Sayer and Wenzel, 2015). On the contrary, the fit became more indefinite as time to maturity increased since the liquidity of the options was lower. Especially with calibrations in the cryptocurrency context, the selected options should be evaluated extra carefully as crypto markets are not generally considered as liquid as more established asset classes as stated by Alexander, Heck, et al. (2022).

When looking at the development of model parameters, first on the list is the mean reversion speed of variance of κ. Timely evolution of κ as well as histograms of the daily changes are given in Figure 6.6.

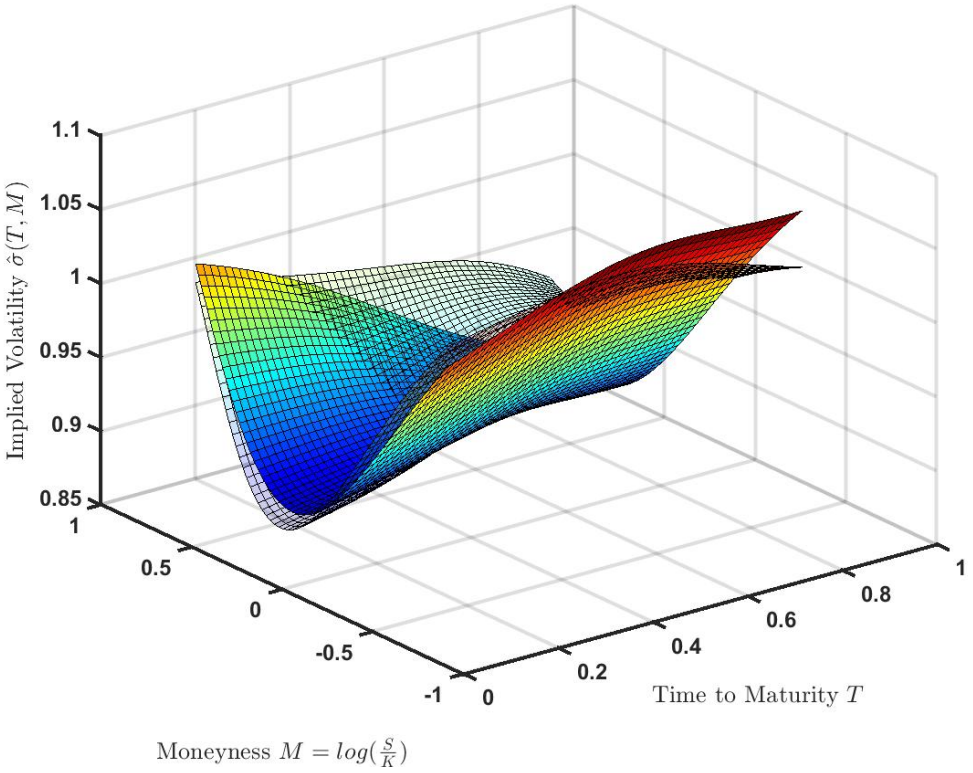

(a) *Heston model*

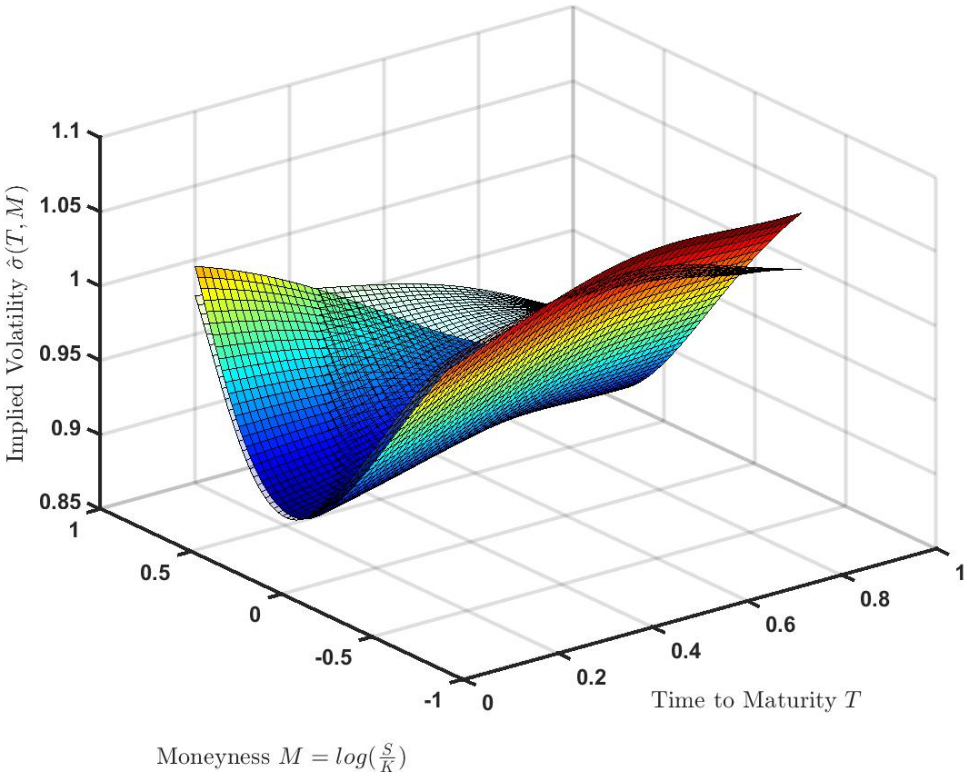

(b) *Bates model*

Figure 6.5. *Model calibrations of both models compared to the quoted implied volatility surface based on the first data snapshot from the 30th of September 2021.*

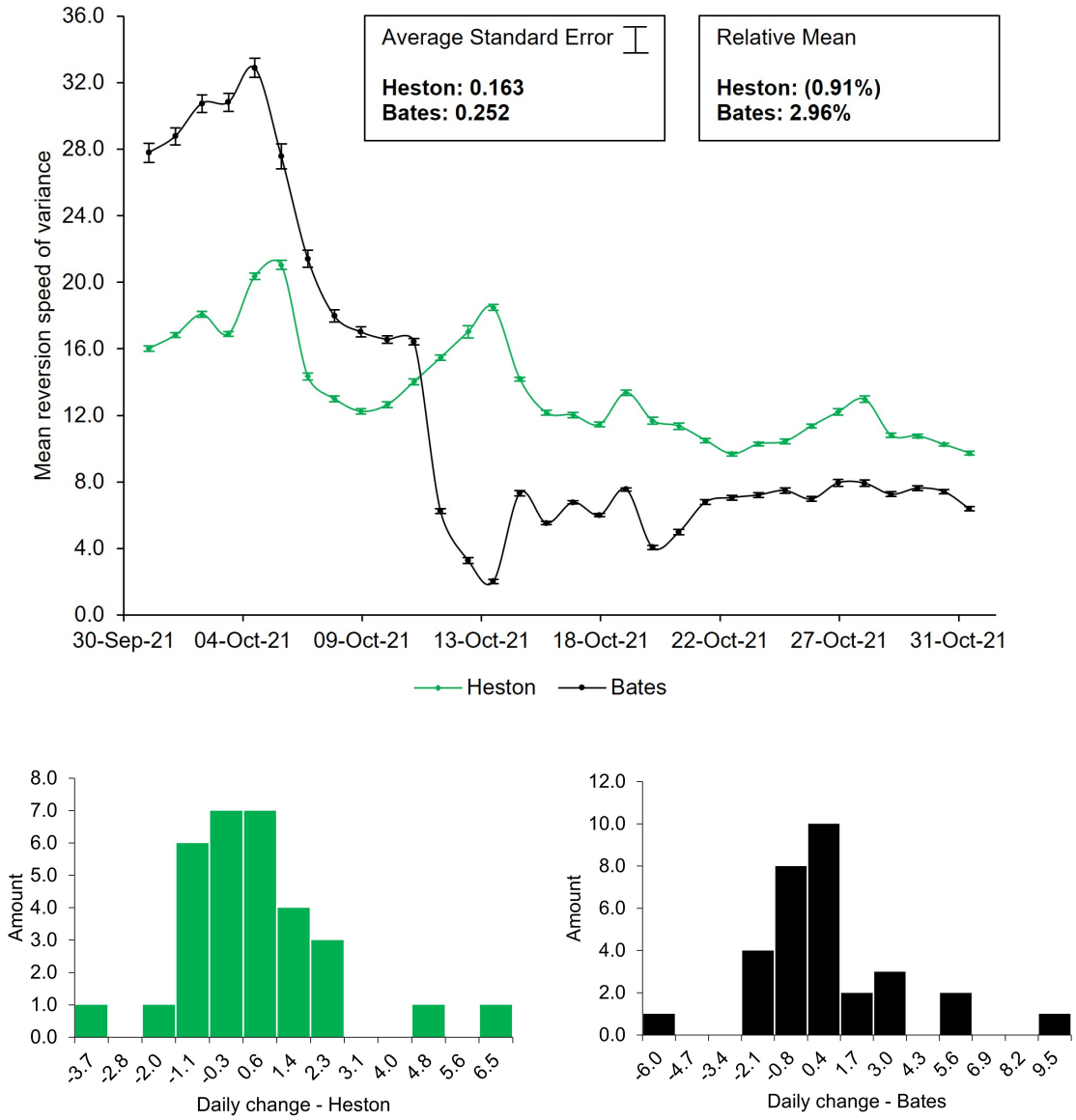

Figure 6.6. *Top: timely evolution with standard errors of the mean reversion speed of variance κ across the review period from the 30th of September 2021 to the 31st of October 2021. Bottom: histograms of the daily changes in terms of the mean change of κ.*

When considering the development of κ for both models, it can be observed that the mean reversion speed of variance was somewhat high for absolute terms regarding each calibration round across the review period. A high value of κ indicates a higher speed of the reversion of the process towards its long-term variance of θ. Moreover, according to Escobar and Gschnaidtner (2016), a higher value of κ also makes out-of-the-money call options more expensive, which can be considered reasonable considering the observed forward skewness of the quoted implied volatility surfaces in Section 6.1. From a cryptocurrency perspective, higher values of κ are also supported by Madan et al.'s (2019) research, where the Heston model calibration to BTC options over time produced

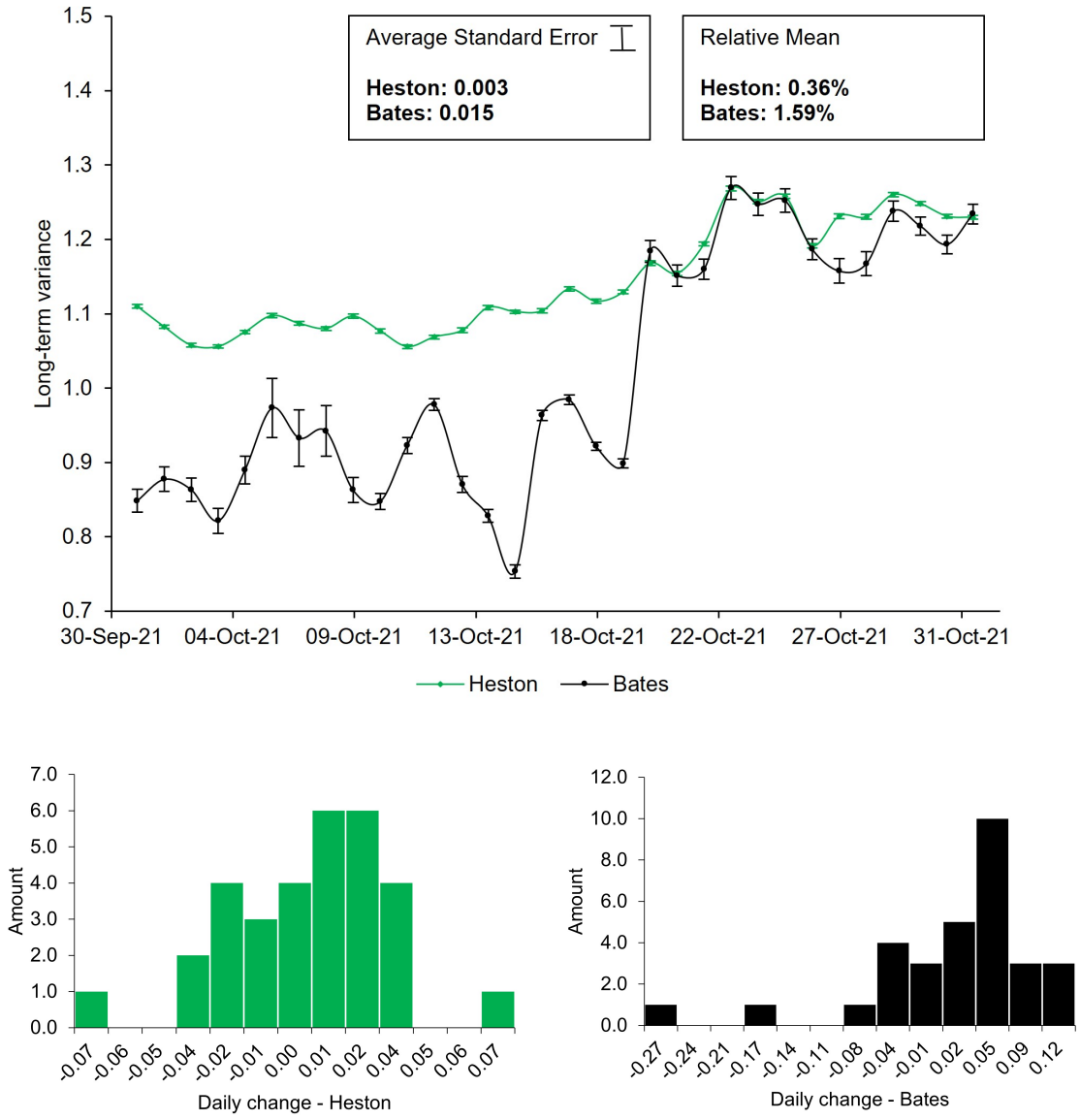

Figure 6.7. *Top: timely evolution and standard errors of the long-term variance θ across the review period from the 30th of September 2021 to the 31st of October 2021. Bottom: histograms of the daily changes in terms of the mean change of θ.*

primarily higher values for κ than for other parameters.

Further, it could be noticed for both models that the average standard error for κ ended up with rather large values in comparison to the other parameters. This practically indicates that the calibration results are not very sensitive to overall changes in κ. Furthermore, timely evolution of κ also reflects some irregularity between the Heston and Bates models. The same behaviour was also observed by Kienitz and Wetterau (2013, p. 509) during their own calibrations. The parameters of the Bates model may follow a different trend because market movements can be compensated by changes in the additional three parameters.

Figure 6.8. *Top: timely evolution and standard errors of the initial variance v_0 across the review period from the 30th of September 2021 to the 31st of October 2021. Bottom: histograms of the daily changes in terms of the mean change of v_0.*

With regards to the long-term variance of θ and the initial variance of v_0, from both models it can be seen that across the review period each of the calibration rounds resulted in a higher value of θ compared to the initial variance of v_0. This indicates that volatility will increase eventually in the future since the estimated value of v_t will approach θ when time t grows towards infinity. A similar connection between θ and v_0 can be recognized from Madan et al.'s (2019) research, where the Heston model calibration to BTC options over time produced also higher values for the long-term variance than for the initial variance. The behaviour of θ and v_0 is illustrated in Figures 6.7 and 6.8.

As can be seen from Figures 6.7 and 6.8, the average standard errors of θ and v_0 were

relatively low for both models. Driven by this, the changes in these parameters can be considered to have a significant effect on the outcome of the calibrations behaving in the opposite way compared to κ. With respect to stability, it was noted that especially the development of θ for the Heston model appeared to be rather stable changing on average 0.36% per day. In other respects, there seemed to be some variation until the 20th of October, after which the movements for both parameters became more stable and aligned between the models.

When it comes to the volatility of volatility η, the development and movements were quite similar to the mean reversion speed of variance of κ. The average standard error of η was relatively large and the observed daily changes were rather big at the beginning of the period levelling off towards the end (Figure 6.9). On a general level, η ended up with quite high values for absolute terms, being in line with Madan et al.'s (2019) study where the Heston model was calibrated to BTC options. As stated by Kienitz and Wetterau (2013, p. 62), high values of η results in an overall higher realized variance and leads to a more volatile behaviour of the price path for the underlying asset. This seems to be reasonable when reflecting on the historical performance and development of bitcoin.

With regards to the correlation of ρ (Figure 6.10), an interesting observation was made. The correlation between the two Wiener processes were positive during the whole review period for both models. As mentioned in Section 4.4 the correlation of ρ impacts on the skewness of the return's distribution, and moreover it defines the skewness of the implied volatility smile. In particular, positive values of ρ cause a positive skew in the return distribution because higher returns go hand in hand with higher volatilities, stretching the right tail of the return distribution. Furthermore, Cížek et al. (2005, p. 173) especially state that positive correlation makes call options more expensive whereas negative correlation accelerates the price of put options.

Nonetheless, there have been relatively few indications of a positive correlation in the literature since typically the correlation between returns and volatility is negative. However, the dynamics of cryptocurrencies differ in many ways from more regular assets. According to Alexander and Imeraj's (2020) article, one feature of bitcoin deviating from equity markets is the volatility of BTC not always being negatively correlated with its returns. This is in line with Hou et al.'s (2020) study on pricing BTC options where the correlation of ρ ends up at positive values with both the Heston and Bates models. The authors noted that the observed non-negative relation between returns and volatility can be possibly explained with the following features: (i) the irregularity of the BTC market, (ii) the price is heavily driven by emotions and sentiments and (iii) the BTC price is not informative since there are no fundamentals allowing the BTC market to define a fair value for bitcoin (Hou et al., 2020). Both of these articles support the results obtained in this thesis.

In other respects, the average standard error of the correlation appeared to be relatively

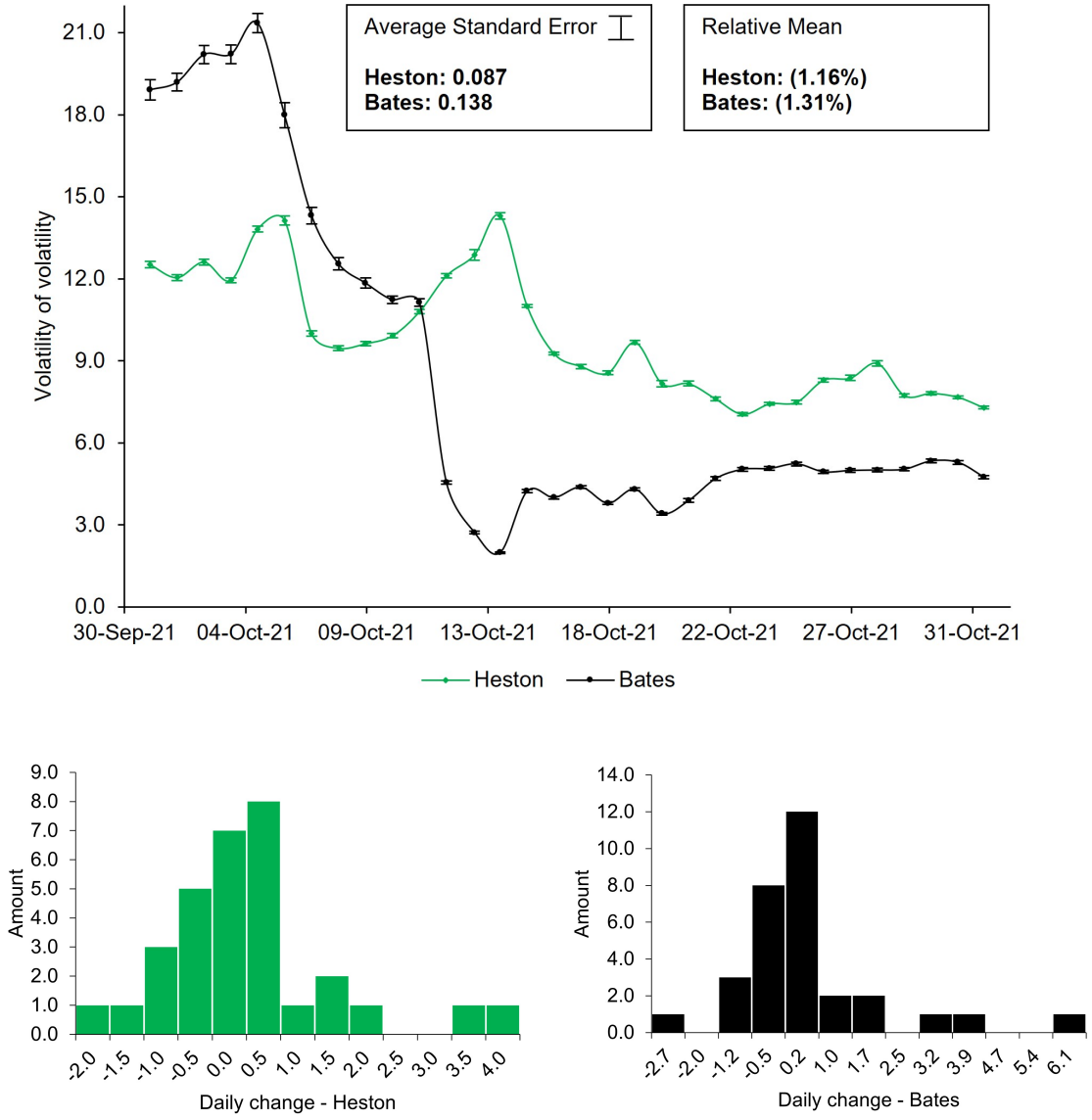

Figure 6.9. *Top: timely evolution and standard errors of the volatility of volatility η across the review period from the 30th of September 2021 to the 31st of October 2021. Bottom: histograms of the daily changes in terms of the mean change of η.*

low for both models. Therefore, the calibration results react sensitively to changes in the correlation ρ having the same characteristics as the long-term variance θ and initial variance v_0.

When it comes to the jump diffusion parameters that are only characteristic for the Bates model, they also provided somewhat interesting outcomes. By including the (i) mean jump size $\overline{k}$, (ii) standard deviation of the jump size δ and (iii) intensity jump parameter λ in the calibration procedure, each calibration round took significantly more time to complete in comparison to the Heston model. Also, the overall variation within the Bates parameters was more noticeable since those additional jump diffusion parameters provided more

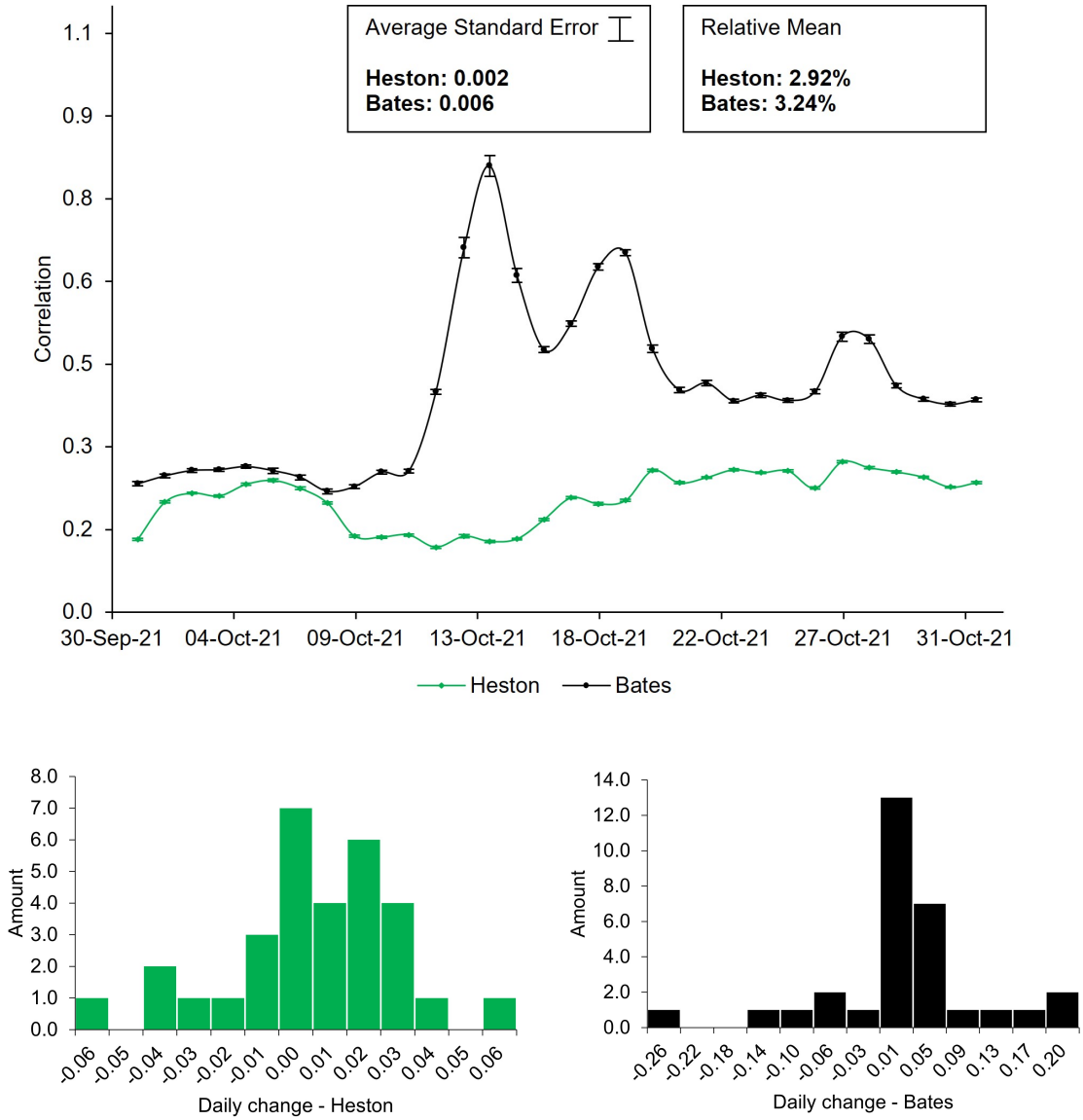

Figure 6.10. *Top: timely evolution and standard errors of the correlation ρ across the review period from the 30th of September 2021 to the 31st of October 2021. Bottom: histograms of the daily changes in terms of the mean change of ρ.*

flexibility to fit the model implied volatilities to the shape of the market IVS.

As can be seen from Figure 6.11, the mean jump size of $\overline{k}$ ended up with a negative value for each calibration round. This indicates that the typical direction of an occurring jump in the price process would be downwards. Furthermore, the standard deviation of the jump size of δ practically remained nearly identical to zero throughout the review period. Since the jump diffusion parameter of δ defines the standard deviation around $\overline{k}$, it indicates that the jump height appears to be rather deterministic without having randomness involved in the jump height development.

In terms of the jump intensity of λ, the development across the review period was some-

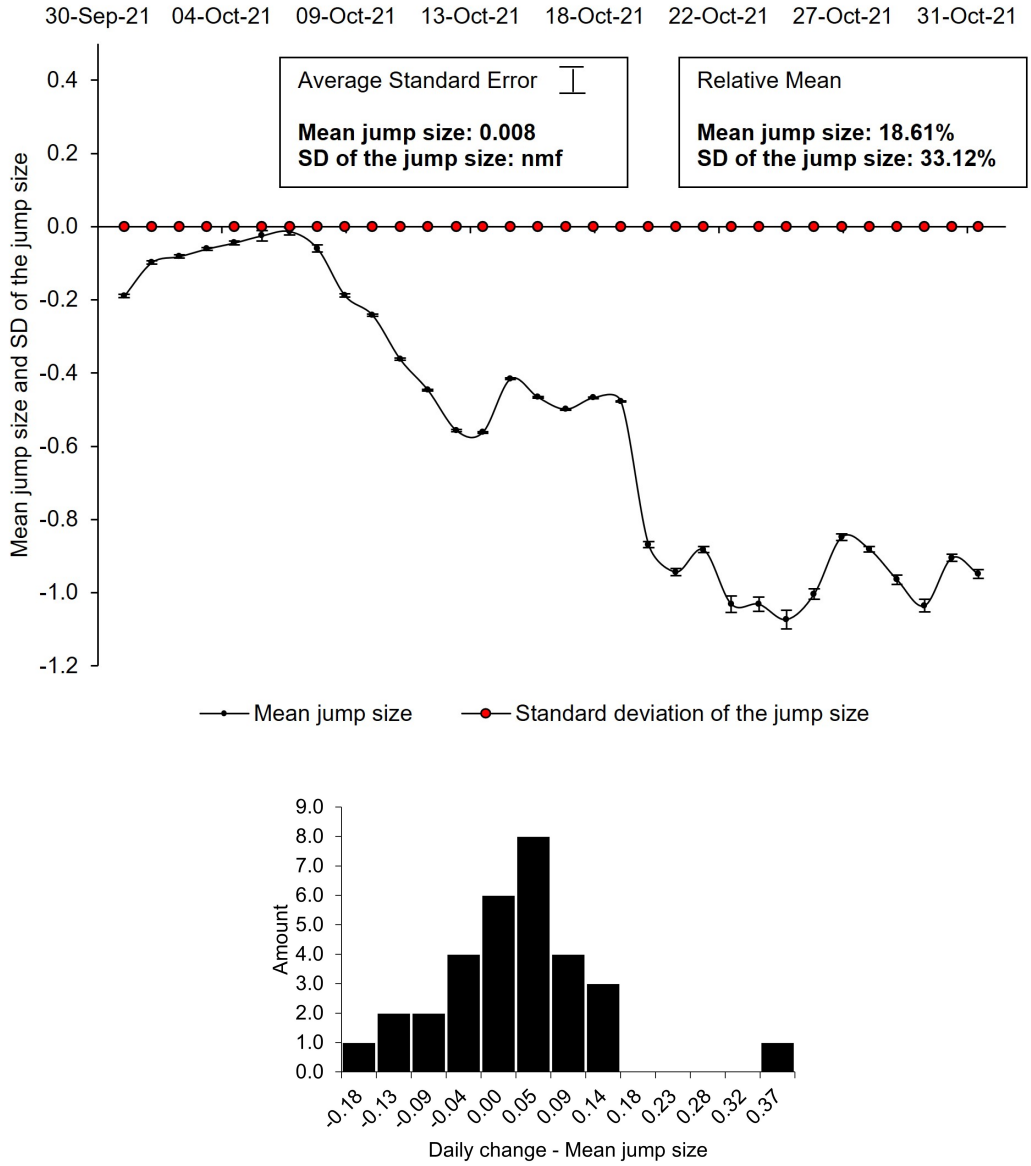

Figure 6.11. *Top: timely evolution and standard errors of the mean jump size $\overline{k}$ across the review period from the 30th of September 2021 to the 31st of October 2021. For illustrative purposes, this Figure also includes the development of the standard deviation of the jump size δ over the review period, although the values remained nearly identical to zero. Bottom: a histogram of the daily changes in terms of the mean change of $\overline{k}$. Note that the daily change histogram for δ has been excluded from the analysis since the obtained values of δ were so close to zero.*

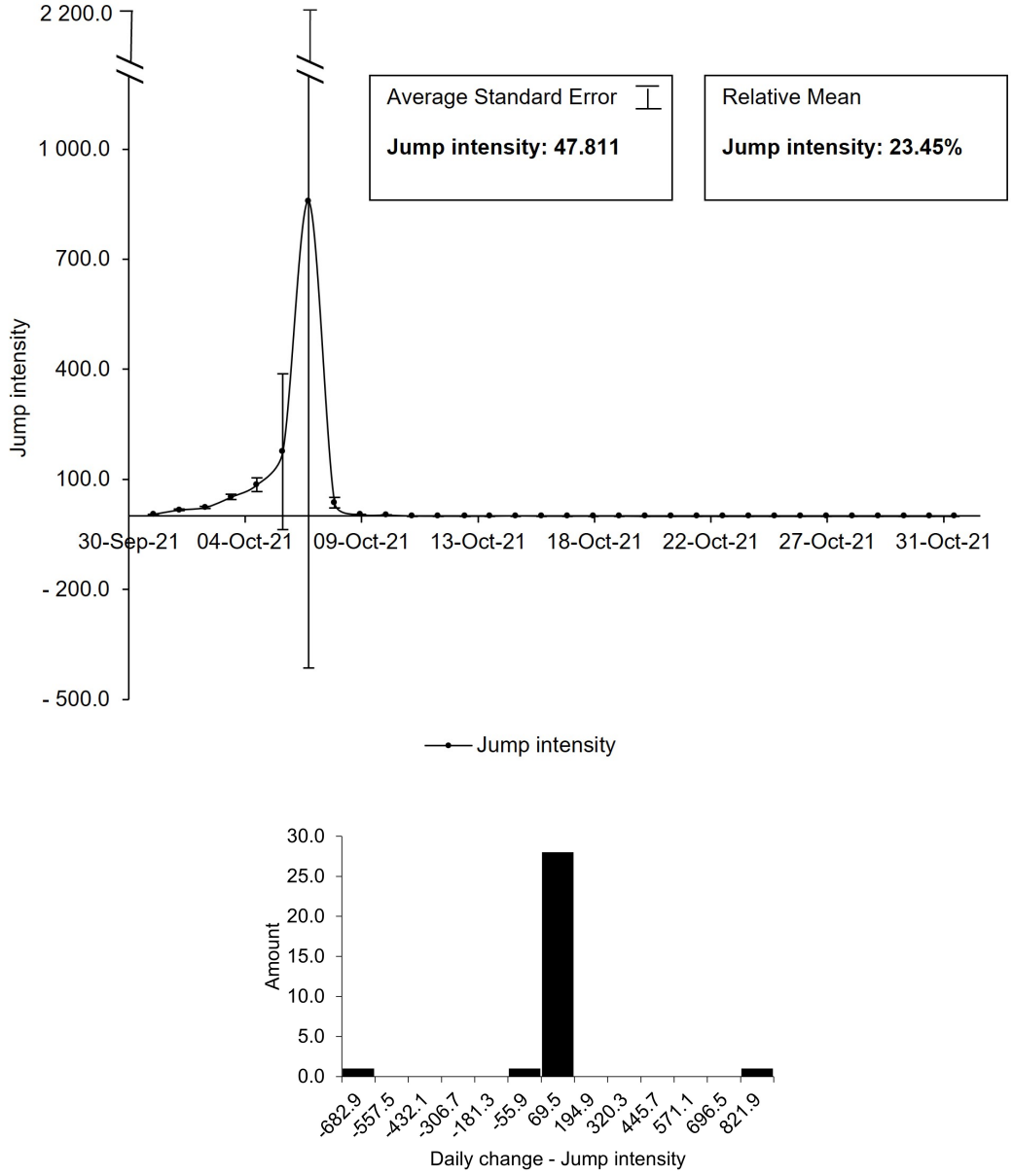

Figure 6.12. *Top: timely evolution of the jump intensity λ across the review period from the 30th of September 2021 to the 31st of October 2021. Bottom: a histogram of the daily changes in terms of the mean change of λ.*

what irregular (Figure 6.12). On absolute terms, the values of λ increased rapidly at the beginning of the review period indicating relatively high frequency of jumps. However, already within the next calibration round, λ behaved the opposite way and dropped significantly, remaining fairly stable towards the end of the period. The observed changes in λ highlight the importance of the input values, which is also emphasized by Escobar and Gschnaidtner (2016). Even though previously calibrated parameters were used as starting values for the next calibration in this thesis, the outcome can be really distorted if market conditions change suddenly causing challenges to the local optimization algorithm to find the true minimum.

For the most part, the obtained results for the jump diffusion parameters were supported by Hou et al.'s (2020) study about pricing BTC options. The authors used a notably higher value for δ compared to the calibrations in this thesis but their estimations for $\overline{k}$ and λ were consistent with the here received results (after λ was levelled off at the end of the review period).

By looking at the average standard errors, it can be observed that the calibration results were also rather sensitive to the variation of the mean jump size of $\overline{k}$. When it comes to λ, the average SE ended up at really high values driven by the rapid changes in the beginning. Even though the calibrated lambda became more stable towards the end of the period, its average standard error of 47.811 was easily the highest in relation to other parameters. With respect to δ, this thesis was unable to reliably determine the standard error as noted in Section 5.5. However, it seemed to vary quite a lot during calibration rounds with little effect on the resulted IV-MSE.

Even though the achieved fit between model and market surfaces across the review period looked rather good for certain options, it neither necessarily means that the calibrated parameters represent true parameters nor that they are suitable in bitcoin option pricing in the long run. As stated in Section 4.1, the calibration process practically always involves some level of model and calibration risk. These risks can be partly managed by (i) performing a sufficient number of re-calibrations, (ii) carrying out an out-of-sample analysis where the calibration will be accomplished again through a data set that was not used in the calibration in the first place or (iii) considering some additional safety margin in the option price to cover potential calibration-related risks as suggested by Guillaume and Schoutens (2012).

In summary, the empirical analysis proceeded as expected and it provided interesting observations about the implied volatility surfaces of bitcoin options as well as model calibrations for the Heston and Bates models. Most of these observations were supported by previous studies from the literature. The main findings and conclusions are summarized in Section 7.1.

7. CONCLUSIONS

7.1 Principal findings

The purpose of this master thesis was to conduct a calibration of asset pricing models to the European-style call options, which use the bitcoin as an underlying asset. Furthermore, this thesis aimed at covering the following research questions, keeping the main focus on the latter one. Firstly, what kind of implied volatility surfaces did European-style bitcoin call options develop, and how did those change across the review period. Secondly, what kind of parameters and mean squared errors were obtained when the Heston and Bates asset pricing models were calibrated against quoted implied volatility surfaces, and how did those parameters and mean squared errors develop throughout the review period.

Based on the constructed implied volatility surfaces, the variation throughout the review period was relatively large even though the review period was only one month long. Despite the previous research on the BTC derivative markets being rather limited, some familiar features were identified from the quoted IV surfaces. During the review period, each IV surface provided a rather clear smile ending in either a fairly symmetrical or forward skewed shape. The smile appeared very clearly for short-term options, whereas it became more and more forward skew shaped as time to maturity increased. A forward skew shape is partly attributable to increased demand for OTM call options to hedge bitcoin's price risk since the crypto market suffers from higher downside risk compared to the normal stock market. Moreover, the observed implied volatility levels within each quoted IV surface were much higher than what normally can be seen with S&P 500 options reflecting a high volatility tendency for bitcoin.

Since the review period was relatively short, a more comprehensive statistical analysis of the differences between the surfaces could not have been carried out for this thesis. However, several factors were identified and reviewed which could possibly explain these differences. Many of these were related to unexpected changes in bitcoin's price since its value fundamentals and return drivers are still rather unclear and not widely acknowledged. Apart from that, bitcoin traders' volatility-motivated demand and risk-averse behaviour may cause impulses in the option supply and demand curves which can lead to rapid changes in the IV surfaces even within a short period of time.

Based purely on the calibration results, both models have capabilities for pricing BTC options especially those with short time to maturities. Even though crypto markets are generally not considered as liquid as more familiar assets, such options with short maturities typically represent high liquidity and thus are likely to reflect market's fair value improving the calibration results. It is noted that by excluding the type of options with relatively low liquidity or alternatively considering weights in calibration, giving more relevancy to ATM options, would have possibly led to better results. Overall, the resulted errors between the IV surfaces were clearly smaller within the strike dimension compared to the maturity dimension. In comparison with the Heston model, the calibrated parameters of the Bates model resulted in a better fit although they encountered more variation and calibration rounds took more time to complete. This was mostly attributable to additional jump diffusion parameters of the Bates model that provided more flexibility to fit the model implied volatilities to the shape of the market IVS.

When observing the calibrated parameters, they did not only reflect a relatively high volatility for bitcoin but also that bitcoin's volatility itself is very volatile. Furthermore, being more or less characteristic of the crypto market, the correlation for both models ended up with positive values across the review period indicating a non-negative relation between returns and volatility. This behaviour deviates from a typical negative leverage effect in equity markets. Based on the jump diffusion parameters of the Bates model, the typical direction of an occurring jump in the price process follows a downward trend. Furthermore, the jump height seems to be rather deterministic without having randomness involved in the jump height development. Moreover, daily average variations in the jump diffusion parameters were more noticeable compared to other parameters.

By looking at the average standard errors, the calibrated parameters such as initial variance v_0, long-term variance θ, correlation ρ as well as mean jump size $\overline{k}$ resulted in relatively small standard errors. Based on these observations, those parameters have a greater impact on the outcomes of the calibration representing greater calibration risk. Therefore, those parameters and their initial values as well as possible restrictions should be considered more precisely compared to the remaining parameters. Overall, it is recommended to re-calibrate the models every time the parameters are used in option pricing to reduce possible calibration risks. This is important especially in this study since the parameters encountered comparatively high variation during the review period.

Since the used review period was quite narrow, the importance of the initial values increases. Perhaps with more accurate initial values for λ and δ, the jump intensity would neither have had a rapid increase in the beginning nor would the standard deviation of the jump size have decreased to nearly identical to zero. On the other hand, this raises a question about the applied optimization algorithm. Especially since previously calibrated parameters were used as starting values for the next calibration, sudden changes in market conditions could cause challenges to the local optimization algorithm to find the true

minimum. Therefore by using global optimization instead of local would have probably led to better calibration results.

All in all, with a longer review period, the development of each parameter could have been evaluated more precisely, and thus produce a better understanding of the behaviour of bitcoin. However, since the literature on crypto derivatives can still be considered rather limited, this thesis may offer new perspectives and insights to practitioners.

7.2 Further research

This thesis gives outlines for further research. First of all, the concluded results should be validated through a longer review period for evaluating possible drivers and patterns behind parameter changes and implied volatility. Moreover, the pricing models of crypto derivatives should be further explored. Even though there are some studies about the valuation of bitcoin options, there are no accurate valuation approaches that would capture the nature of cryptocurrency and define the values of crypto derivatives in a consistent fashion.

Another important topic for further research would be to build a coherent consensus around a model calibration process within the cryptocurrency context. It is noted that a model calibration process in equity option pricing is a widely reviewed subject and the main fundamentals such as choosing the relevant input values and loss function have been studied rather closely in previous studies. However, a similar comprehensive and detailed analysis has not been done from a cryptocurrency perspective. Since bitcoin is known for its exceptional and unregulated monetary policy as well as highly sensitive price development in the environment of a limited amount of currencies, using traditional calibration methods does not necessarily make sense. This topic could provide more support to the already complex valuation process.

REFERENCES

Albrecher, H., Mayer, P., Schoutens, W., & Tistaert, J. (2007). The little heston trap. *Wilmott*, (1), 83–92.

Alexander, C., Chen, D., & Imeraj, A. (2021). Inverse options in a black-scholes world. *SSRN Electronic Journal*.

Alexander, C., Deng, J., Feng, J., & Wan, H. (2022). Net buying pressure and the information in bitcoin option trades. *Journal of Financial Markets*, *63*, 100764–.

Alexander, C., Heck, D. F., & Kaeck, A. (2022). The role of binance in bitcoin volatility transmission. *Applied Mathematical Finance*, *29*(1), 1–32.

Alexander, C., & Imeraj, A. (2020). Bvin: The bitcoin volatility index.

Aste, T. (2019). Cryptocurrency market structure: Connecting emotions and economics. *Digital Finance*, *1*(1-4), 5–21.

Athey, S., Parashkevov, I., Sarukkai, V., & Xia, J. (2016). Bitcoin pricing, adoption, and usage: Theory and evidence. *IDEAS Working Paper Series from RePEc*.

Bams, D., Lehnert, T., & Wolff, C. C. P. (2009). Loss functions in option valuation: A framework for selection. *Management Science*, *55*(5), 853–862.

Bandi, F., & Renò, R. (2016). Price and volatility co-jumps. *Journal of financial economics*, *119*(1), 107–146.

Bates, D. S. (1996). Jumps and stochastic volatility: Exchange rate processes implicit in deutsche mark options. *The Review of Financial Studies*, *9*(1), 69–107.

Bhambhwani, S., Delikouras, S., & Korniotis, G. (2019). Do fundamentals drive cryptocurrency prices? *IDEAS Working Paper Series from RePEc*.

Bistarelli, S., Cretarola, A., Figà-Talamanca, G., & Patacca, M. (2019). Model-based arbitrage in multi-exchange models for bitcoin price dynamics. *Digital finance*, *1*(1-4), 23–46.

Black, F., & Scholes, M. (1973). The pricing of options and corporate liabilities. *The Journal of political economy*, *81*(3), 637–654.

Bollen, N. P., & Whaley, R. E. (2004). Does net buying pressure affect the shape of implied volatility functions? *The Journal of Finance*, *59*(2), 711–753.

Borri, N. (2019). Conditional tail-risk in cryptocurrency markets. *Journal of Empirical Finance*, *50*, 1–19.

Boyle, P., & McDougall, J. (2019). *Trading and pricing financial derivatives*. Walter De Gruyter Inc.

Büchel, P., Kratochwil, M., Nagl, M., & Rösch, D. (2022). Deep calibration of financial models: Turning theory into practice. *Review of Derivatives Research*, *25*(2), 109–136.

Cao, M., & Celik, B. (2021). Valuation of bitcoin options. *Journal of Futures Markets*, *41*(7), 1007–1026.

Carr, P., & Madan, D. (1999). Option valuation using the fast fourier transform. *Journal of computational finance*, *2*(4), 61–73.

Chaum, D. (1983). Blind signatures for untraceable payments. *Advances in Cryptology: Proceedings of Crypto 82*, 199–203.

Christoffersen, P., Heston, S., & Jacobs, K. (2009). The shape and term structure of the index option smirk: Why multifactor stochastic volatility models work so well. *Management Science*, *55*(12), 1914–1932.

Cížek, P., Härdle, W., & Weron, R. (2005). *Statistical tools for finance and insurance*. Springer.

CoinDesk. (n.d.). *Coindesk btc price index*. Retrieved March 23, 2023, from https://www.coindesk.com/price/bitcoin/.

CoinMarketCap. (n.d.). *Bitcoin to usd historical data*. Retrieved March 22, 2023, from https://coinmarketcap.com/currencies/bitcoin/.

Cont, R. (2006). Model uncertainty and its impact on the pricing of derivative instruments. *Mathematical finance*, *16*(3), 519–547.

Cont, R., & Da Fonseca, J. (2002). Dynamics of implied volatility surfaces. *Quantitative finance*, *2*(1), 45–60.

Cont, R., & Tankov, P. (2004). *Financial modelling with jump processes*. CRC Press.

Cox, J. C., Ingersoll, J. E., & Ross, S. A. (1985). A theory of the term structure of interest rates. *Econometria*, *53*(2), 385–407.

Cretarola, A., Figà-Talamanca, G., & Patacca, M. (2020). Market attention and bitcoin price modeling: Theory, estimation and option pricing. *Decisions in Economics and Finance*, *43*(1), 187–228.

De Vries, A. (2020). Bitcoin's energy consumption is underestimated: A market dynamics approach. *Energy Research & Social Science*, *70*, 101721–.

Dorn, J. A. (2017). *Monetary alternatives: Rethinking government fiat money.* Cato Institute.

Duffie, D., Pan, J., & Singleton, K. (2000). Transform analysis and asset pricing for affine jump-diffusions. *Econometrica*, *68*(6), 1343–1376.

Escobar, M., & Gschnaidtner, C. (2016). Parameters recovery via calibration in the heston model: A comprehensive review. *Wilmott*, *2016*(86), 60–81.

Feller, W. (1951). Two singular diffusion problems. *Annals of mathematics*, *54*(1), 173–182.

Fengler, M. R. (2005). *Semiparametric modeling of implied volatility*. Springer.

Fiorentini, G., Leon, A., & Rubio, G. (2002). Estimation and empirical performance of heston's stochastic volatility model: The case of a thinly traded market. *Journal of empirical Finance*, *9*(2), 225–255.

Franco, P. (2014). *Understanding bitcoin: Cryptography, engineering and economics*. Wiley.

Gkillas, K., & Longin, F. (2019). Is bitcoin the new digital gold? evidence from extreme price movements in financial markets. *SSRN Electronic Journal*.

Guillaume, F., & Schoutens, W. (2012). Calibration risk: Illustrating the impact of calibration risk under the heston model. *Review of Derivatives Research*, *15*(1), 57–79.

Härdle, W. K., Harvey, C. R., & Reule, R. C. (2020). Understanding cryptocurrencies. *Journal of Financial Econometrics*, *18*(2), 181–208.

Hayes, A. S. (2017). Cryptocurrency value formation: An empirical study leading to a cost of production model for valuing bitcoin. *Telematics and Informatics*, *34*(7), 1308–1321.

Heston, S. L. (1993). A closed-form solution for options with stochastic volatility with applications to bond and currency options. *The review of financial studies*, *6*(2), 327–343.

Hoang, L. T., & Baur, D. G. (2020). Forecasting bitcoin volatility: Evidence from the options market. *Journal of Futures Markets*, *40*(10), 1584–1602.

Hou, A. J., Wang, W., Chen, C. Y., & Härdle, W. K. (2020). Pricing cryptocurrency options. *Journal of Financial Econometrics*, *18*(2), 250–279.

Hull, J. C. (2012). *Options, futures, and other derivatives* (8th edition). Pearson Education.

Iacus, S. M. (2011). *Option pricing and estimation of financial models with r* (1st edition). Wiley.

Ibe, O. C. (2013). *Markov processes for stochastic modeling* (2nd edition). Elsevier.

Itô, K. (1951). *On stochastic differential equations*. Memoirs of the American Mathematical Society.

Jalan, A., Matkovskyy, R., & Aziz, S. (2021). The bitcoin options market: A first look at pricing and risk. *Applied Economics*, *53*(17), 2026–2041.

Judd, S., & Judd, C. (2011). *The mbr book principles and applications of membrane bioreactors for water and wastewater treatment* (2nd edition). Elsevier.

Kienitz, J., & Wetterau, D. (2013). *Financial modelling: Theory, implementation and practice (with matlab source)*. Wiley.

Köchling, G., Müller, J., & Posch, P. N. (2019). Does the introduction of futures improve the efficiency of bitcoin? *Finance Research Letters*, *30*, 367–370.

Krückeberg, S., & Scholz, P. (2020). Decentralized efficiency? arbitrage in bitcoin markets. *Financial Analysts Journal*, *76*(3), 135–152.

Küfeoğlu, S., & Özkuran, M. (2019). Bitcoin mining: A global review of energy and power demand. *Energy Research & Social Science*, *58*, 101273–.

Lagarias, J. C., Reeds, J. A., Wright, M. H., & Wright, P. E. (1998). Convergence properties of the nelder–mead simplex method in low dimensions. *SIAM Journal on optimization*, *9*(1), 112–147.

Lipovyanov, P. (2019). *Blockchain for business 2019: A user-friendly introduction to blockchain technology and its business applications* (1st edition). Packt Publishing Ltd.

Liu, S., Oosterlee, C. W., & Bohte, S. M. (2019). Pricing options and computing implied volatilities using neural networks. *Risks*, *7*(1), 16–.

Liu, Y., Tsyvinski, A., & Wu, X. (2022). Common risk factors in cryptocurrency. *The Journal of Finance*, *77*(2), 1133–1177.

Madan, D. B., Reyners, S., & Schoutens, W. (2019). Advanced model calibration on bitcoin options. *Digital Finance*, *1*(1-4), 117–137.

Makarov, I., & Schoar, A. (2020). Trading and arbitrage in cryptocurrency markets. *Journal of financial economics*, *135*(2), 293–319.

Merton, R. C. (1976). Option pricing when underlying stock returns are discontinuous. *Journal of financial economics*, *3*(1-2), 125–144.

Mikhailov, S., & Nögel, U. (2004). Heston's stochastic volatility model: Implementation, calibration and some extensions. *Wilmott magazine*.

Mir, U. (2020). Bitcoin and its energy usage: Existing approaches, important opinions, current trends, and future challenges. *KSII Transactions on Internet and Information Systems*, *14*(8), 3243–3256.

Nakamoto, S. (2008). Bitcoin: A peer-to-peer electronic cash system. *Decentralized Business Review*, 21260–.

Nelder, J. A., & Mead, R. (1965). A simplex method for function minimization. *The computer journal*, *7*(4), 308–313.

Pachamanova, D. A., & Fabozzi, F. J. (2010). *Simulation and optimization in finance: Modeling with matlab, @risk, or vba* (Vol. 173). Wiley.

Raj, K. (2019). *Foundations of blockchain: The pathway to cryptocurrencies and decentralized blockchain applications*. Packt Publishing, Limited.

Ratcliff, R., & Tuerlinckx, F. (2002). Estimating parameters of the diffusion model: Approaches to dealing with contaminant reaction times and parameter variability. *Psychonomic bulletin & review*, *9*(3), 438–481.

Rouah, F. D. (2015). *The heston model and its extensions in vba* (1st edition). Wiley.

Santos-Alborna, A. (2021). *Understanding cryptocurrencies : Bitcoin, ethereum, and altcoins as an asset class.* (1st edition). Business Expert Press.

Saunders, M., Lewis, P., & Thornhill, A. (2019). *Research methods for business students* (8th edition). Pearson Education.

Sayer, T., & Wenzel, J. (2015). From model to application: Calibration to market data. Springer International Publishing.

Sepp, A. (2003). Fourier transform for option pricing under affine jump-diffusions: An overview. *SSRN Electronic Journal*.

Simon, C. P., & Blume, L. (1994). *Mathematics for economists*. Norton.

Stoll, H. R. (1969). The relationship between put and call option prices. *The Journal of Finance*, *24*(5), 801–824.

Teneng, D. (2011). Limitations of the black-scholes model. *International Research Journal of Finance and Economics*, *68*, 99–102.

Teng, H.-W., & Härdle, W. K. (2022). Financial analytics of inverse btc options in a stochastic volatility world. *SSRN Electronic Journal*.

Verousis, T., ap Gwilym, O., & Voukelatos, N. (2016). Commonality in equity options liquidity: Evidence from european markets. *The European journal of finance*, *22*(12), 1204–1223.

Yan, L., & Jianhui, Y. (2016). Option pricing model based on newton-raphson iteration and rbf neural network using implied volatility. *Canadian Social Science*, *12*(8), 25–29.

Yu, F., Rudd, R., Baker, C., Mashalaba, Q., Mavuso, M., & Schlögl, E. (2018). Quantifying the model risk inherent in the calibration and recalibration of option pricing models. *arXiv*.

Zhang, S., Zhou, X., Pan, H., & Jia, J. (2019). Cryptocurrency, confirmatory bias and news readability–evidence from the largest chinese cryptocurrency exchange. *Accounting & Finance*, *58*(5), 1445–1468.

Zhang, W., Li, Y., Xiong, X., & Wang, P. (2021). Downside risk and the cross-section of cryptocurrency returns. *Journal of Banking & Finance*, *133*, 106246–.

Zulfiqar, N., & Gulzar, S. (2021). Implied volatility estimation of bitcoin options and the stylized facts of option pricing. *Financial Innovation*, *7*, 1–30.